

NEUTRINOS IN HOT AND DENSE MEDIA

Samina Masood

Dept. of Physical and Applied Sciences

University of Houston Clear Lake

Houston, TX



Outline

- How to define a hot and dense medium.
- Development of statistical quantum field theory for QED.
- Renormalization of QED using perturbation theory.
- Statistical corrections to the propagating particles.
- Renormalized parameters of QED are treated as effective parameters of the theory.
- Properties of the medium are determined from the particle behavior.
- How neutrinos can couple with the magnetic field (neutral particle).
- Results should be incorporated in experimental/observational data analysis.
- Then application to astrophysics, cosmology and reactor physics.



Introduction

- Interacting fluid media is considered
- Interactions are described as gauge theories
- Renormalization can be proved using
 - Perturbative approach (individual particle approach)
 - Effective potential approach (collective approach)
- Perturbation is described like a series expanded in powers of the coupling constant.
- One loop in Feynman diagrams correspond to a single power of the coupling constant in perturbation theory.



Motivation

- Early Universe (around nucleosynthesis)
light particles at very high temperature
($T \sim 10^{10}$ K or above)
- Astronomical Objects super-massive stars have
densities $\sim 10^{14} - 10^{16}$ g/cm³
 $T \sim 10^{10} - 10^{12}$ K
- Magnetic field B is too strong to be ignored in neutron stars and magnetars
 $B \sim 10^{14}$ G
 $\mu_e \sim 200$ MeV ($1\text{MeV} = 10^{10}$ K)



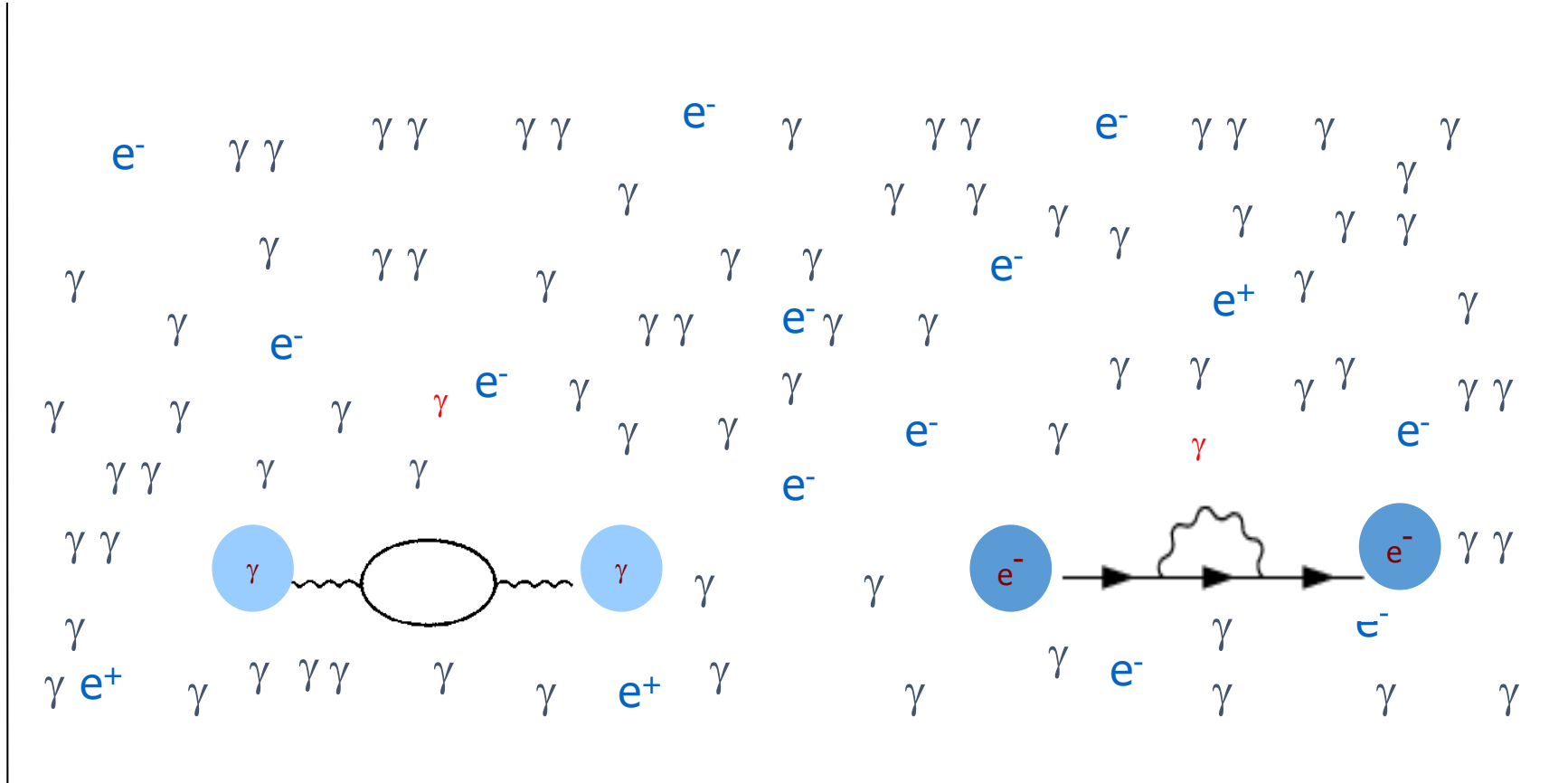
Why the medium effects are required

Calculation of QED parameters at extremely high temperature showed that

- QED coupling becomes a function of temperature at the second order of perturbation whereas the first order contributions vanish at low temperature. However the high density effect is non-zero.
- First order perturbation changes the electric permittivity, magnetic permeability and other electromagnetic properties of the medium.
- First order perturbations at extremely high densities and low temperatures indicate the dependence of medium properties on the density or chemical potential of the medium.
- So the electromagnetic properties of a highly dense medium may lead to interesting results, if studied using QED.
- Fluid equations and fluid parameters modification with QED may be interesting .
- Phase transitions between classical fluids/plasmas, relativistic plasmas and superfluids
- Latest discovery of superfluid in the core of neutron star supported the idea that fluid phase depend on the ratio of parameters and not on a single parameter.



Heat Bath



Finite Temperature and Density Effects

- All the physical processes take place in a heat bath comprising all kind of relevant hot particles and antiparticles instead of a vacuum, through the radiative corrections. The probability of exchange of virtual particles with the real particles in the background is incorporated.
- Feynman rules of vacuum theories are used and the basic principles remain unchanged.
- In quantum field theory, the thermal background effects are incorporated via the Fermion and boson propagators only
- Spin statistics of the particles and their properties in vacuum are incorporated as it is.
- The renormalization of electric mass and charge through the self-energy calculation in different frameworks change the physically measurable quantities.



Comparison between formalisms

REAL TIME FORMALISM

- Gauge invariant exists is induced by hand at the expense of Lorentz invariance.
- Integration on initial and final states hide the path of the system.
- Hard thermal loops appear.
- Segregation is possible between vacuum and statistical contributions, especially at the one loop level.
- Can go to any order of perturbation. But if the perturbative series is convergent and can be truncated wherever, it make sense.
- Renormalizability---Order by order cancellation of singularities can be shown.
- QED works very well with perturbative analysis. So this approach is preferred for the study of electromagnetic properties.

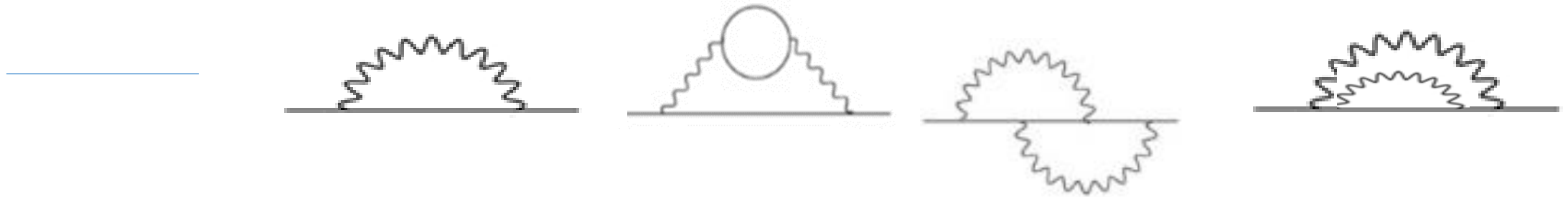
IMAGINARY TIME FORMALISM

- Gauge invariance breaks
- Summation over intermediate states—gives information about the path of the system
- No hard loops
- Statistical effects cannot be separated from the vacuum values.
- All orders of perturbation have to be included.
- Singularities of all orders are cancelled at the same time.
- Only applicable to systems in thermal equilibrium.
- Preferred for non-perturbative analysis of theories where perturbative series does not converge.



Example of Loop diagrams in QED

Self-energy



Vacuum Polarization



$$D_{\mu\nu}(P) = -g_{\mu\nu} \left[\frac{1}{P^2 + i\eta} - i\Gamma_b(P) \right],$$

$$S(P) = (\not{P} + m_0) \left[\frac{1}{P^2 - m_0^2 + i\eta} + i\Gamma_f(P) \right]$$

$$\Gamma_b(P) = 2\pi\delta(P^2)n_b(P),$$

$$\Gamma_f(P) = 2\pi\delta(P^2 - m_0^2)[\theta(P_0)n_f^+(P) + \theta(-P_0)n_f^-(P)].$$

$$\{u=(1,0,0,0)\}$$

$$\beta = \frac{1}{T}$$

Fermion propagator

$$S_B(p) = (\not{p} - m) \left\{ \frac{i}{p^2 - m^2 + i\epsilon} - 2\pi\delta(p^2 - m^2)n_F(E_p) \right\},$$

$$n_F(E_p) = \frac{1}{e^{\beta(p \cdot u)} + 1},$$

Boson Propagator

$$D_B^{\mu\nu}(p) = \left[\frac{i}{k^2 + i\epsilon} - 2\pi\delta(k^2)n_B(k) \right]$$

$$n_B(E_k) = \frac{1}{e^{\beta(k \cdot u)} - 1},$$

J. F. Donoghue and B. R. Holstein, Phys. Rev. D28 (1983) 340. <https://journals.aps.org/prd/abstract/10.1103/PhysRevD.28.340>

Edward J. Levinson and David H. Boal, Phys. Rev. D 31, 3280 (1985)

<https://journals.aps.org/prd/abstract/10.1103/PhysRevD.31.3280>



Renormalization of Gauge Theories

Gauge theories are major interactions theories

Quantum Electrodynamics(QED) is the only abelian gauge (interaction) theory

Renormalization is a procedure to remove singularities of gauge theories

QED coupling is smaller than one in vacuum and the perturbative series converges.

Order by order cancellation of singularities is studied in perturbation theory.

Application of perturbation theory can be used to study QED in statistical medium (described by its composition, temperature, density and magnetic field)



Renormalization Constants of QED

$$\Sigma(p) = A(p)E\gamma_0 - B(p)p \cdot \gamma - C(p)$$

where $A(p)$, $B(p)$, and $C(p)$ are the relevant coefficients and are modified at FTD

$$S^{-1}(p) = (1-A)E\gamma^0 - (1-B)p \cdot \gamma - (m-C), \quad m_{phys} \equiv m + \delta m^{(1)} + \delta m^{(2)}$$

$$\frac{1}{\not{p} - m + i\epsilon} \longrightarrow \frac{Z_2^{-1}}{\not{p} - m + i\epsilon}, \quad Z_2^{-1} = 1 - A = 1 - \frac{\partial \Sigma(p)}{\partial \not{p}}$$



Self-energy of electron interactions

- Electrons have a higher physical mass than the electron rest mass due to interactions with its own electric field

- Self-energy/selfenergy 

- Perturbation in vacuum give the additional mass correction due to vacuum fluctuations and thermal energy.

- Renormalized mass = Physical mass of electron

$$m_R \equiv m_{phys} = m + \delta m(T = 0) + \delta m(T), \quad m_{phys} \cong m + \delta m^{(1)} + \delta m^{(2)} + \dots$$

- New temperature dependent infrared singularities appear due to photon loop
- At high temperatures no additional ultraviolet singularities appear and distribution function provides a cutoff.



First-Order Correction

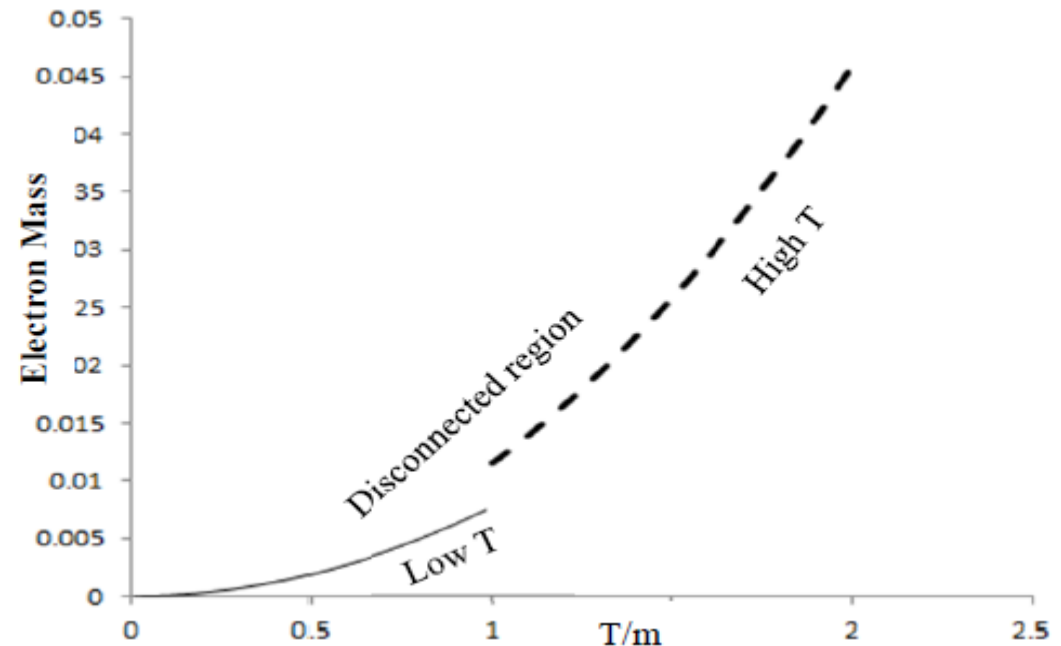
- Low temperature limit $\frac{\delta m}{m} \xrightarrow{T \ll m} \frac{\alpha \pi T^2}{3m^2}$.

- High temperature limit

$$\frac{\delta m}{m} \xrightarrow{T \gg m} \frac{\alpha \pi T^2}{2m^2}$$

- Difference

$$\Delta\left(\frac{\delta m}{m}\right) = \pm \frac{\alpha \pi T^2}{6m^2} = \pm 3.8 \times 10^{-3} \frac{T^2}{m^2}$$



$$\frac{\delta m}{m}(T, \mu) \approx \frac{\alpha \pi T^2}{3m^2} \left[1 - \frac{6}{\pi^2} c(m\beta, \mu) \right] + \frac{2\alpha T}{\pi m} a(m\beta, \mu) - \frac{3\alpha}{\pi} b(m\beta, \mu).$$

$$Z_2^{-1}(T, \mu) = Z_2^{-1}(T = 0, \mu) - \frac{2\alpha}{\pi} \int \frac{dk}{k} n_B(k) - \frac{5\alpha}{\pi} b(m\beta, \mu) + \frac{\alpha T^2}{\pi E^2 v} \ln \frac{1-v}{1+v} \times \left[c(m\beta, \mu) - \frac{\pi^2}{6} - \frac{m}{T} a(m\beta, \mu) \right]$$

$$Z_3(T, \mu) \approx 1 + \frac{\alpha T^2}{6m^2} \left[\frac{ma(m\beta, \mu)}{T} - c(m\beta, \mu) + \frac{1}{4} \left(m^2 + \frac{\omega^2}{3} b(m\beta, \mu) \right) \right]$$

$$Ei(x) = \int_{-x}^{\infty} \frac{e^{-t} dt}{t}$$

$$a(m\beta, \pm\mu) = \ln(1 + e^{-(m\pm\mu)\beta})$$

$$b(m\beta, \pm\mu) = \sum_{n=1}^{\infty} (-1)^n e^{\mp n\beta\mu} Ei(-nm\beta)$$

$$c(m\beta, \pm\mu) = \sum_{n=1}^{\infty} \frac{(-1)^n}{n^2} e^{-n(m\pm\mu)\beta}$$

Ahmed, K. and Masood, S.S. (1987) Physical Review D, 35, 1861

Ahmed, K. and Masood, S.S.: Phys. Rev. D 35, (1987) 4020-4023.



In the high chemical-potential limit ($T < m < \mu$), we obtain

$$a(m\beta, -\mu) = \mu - m - \sum_{l=0}^{\infty} \frac{(-1)^l}{\mu^l} \sum_{n=1}^{\infty} \frac{(-1)^n}{(n\beta)^{1-l}} e^{-n\beta(m-\mu)}$$

$$b(m\beta, -\mu) = \ln(\mu/m)$$

$$c(m\beta, -\mu) = \frac{\mu^2 - m^2}{2} - \sum_{l=0}^{\infty} \frac{(-1)^l}{\mu^l} \sum_{n=1}^{\infty} \frac{(-1)^n}{(n\beta)^l} e^{-n\beta(m-\mu)}$$

At chemical potential equal to electron mass it gives zero contribution and only thermal corrections can be obtained for high temperatures

Masood, S.S. (1993) Physical Review D, 47, 648. <https://journals.aps.org/prd/issues/47/2>

Samina Masood and Iram Saleem, IJMPA, Vol. 32, No. 15 (2017)



Electron mass as a function of chemical potential

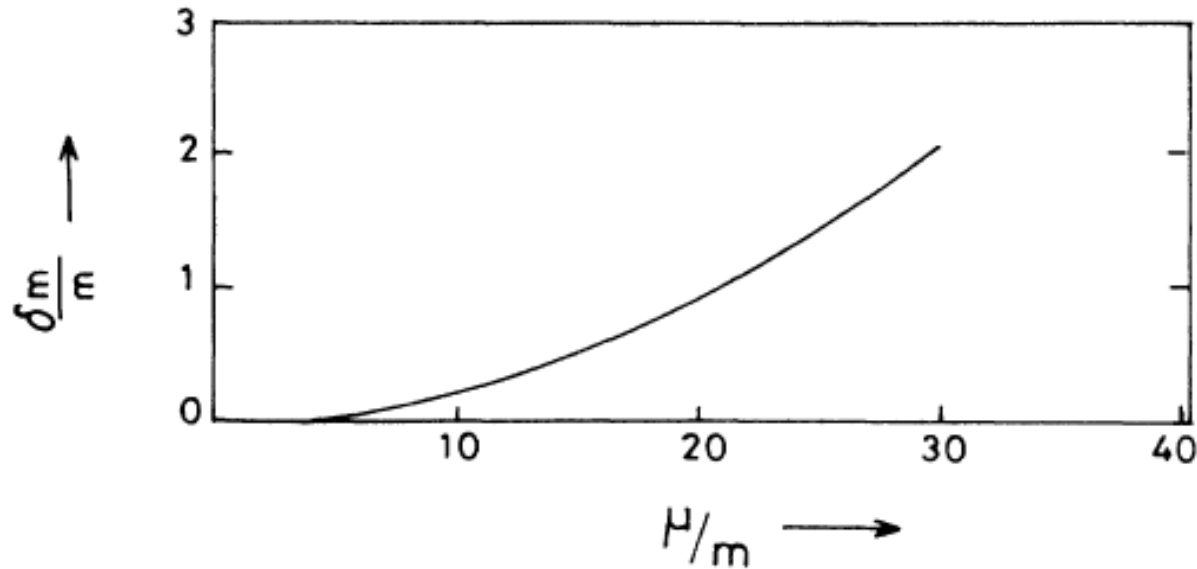


FIG. 1. $\delta m / m$ is plotted against the chemical potential in the limit $T \rightarrow 0$, in the rest frame of electron. It can be clearly seen that $\delta m / m$ increases with the increase in μ / m values.



Two-loop corrections to Electron Selfmass

$$\delta m_{\beta}^{(2)} = \frac{1}{m} (\Sigma_{T=0}^{(1)} + \Sigma_{T \neq 0}^{(1)}) (\delta m_{T=0}^{(1)} + \delta m_{T \neq 0}^{(1)})$$

$T \ll m$

$$m_{\text{phys}}^2 = m_0^2 + \frac{2\alpha}{3} \pi T^2 + \frac{2}{3} \alpha^2 T^2 \left\{ 35 + \frac{3}{v} \ln \frac{1+v}{1-v} + 8 \left[\gamma + \ln 2 + \frac{6}{\pi^2} \sum_{n=1}^{\infty} \frac{1}{n^2} \ln \left[\frac{nm}{T} \right] \right] \right\},$$

$\gamma = 0.5772$ Euler-Mascheroni constant

Qader, M., Masood, S.S. and Ahmed, K. (1991) Physical Review D, 44, 3322.

Qader, M., Masood, S.S. and Ahmed, K. (1992) Physical Review D, 46, 5633



Two-loop corrections to Electron Selfmass

Initially , it was proposed that at high temperature we may write thermal effect in the series expansion

$$\Sigma_{\beta}(p) \sim T \sum_{n=1} c_n \alpha^n \left[\frac{T}{p} \ln \frac{E+p}{E-p} \right]^n$$

But it was later found to be much more complicated

Duane A. Dicus, David Down, and Edward W. Kolb, Nucl. Phys. B223, 525 (1983).

Qader, M., Masood, S.S. and Ahmed, K. (1991) Physical Review D, 44, 3322. <https://journals.aps.org/prd/abstract/10.1103/PhysRevD.44.3322>

Qader, M., Masood, S.S. and Ahmed, K. (1992) Physical Review D, 46, 5633. <https://journals.aps.org/prd/abstract/10.1103/PhysRevD.46.5633>

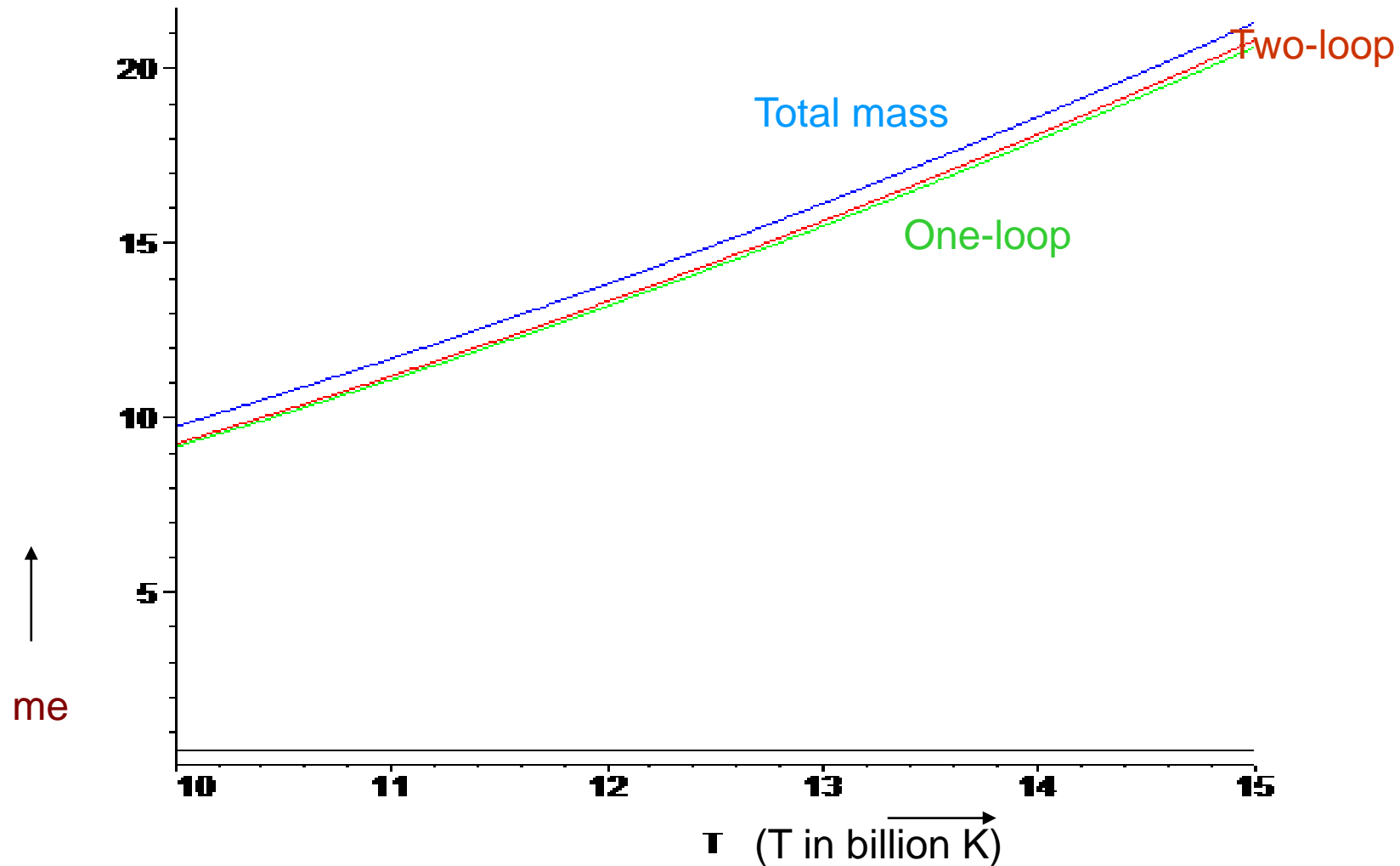


$$\frac{\delta m^{(2)}}{m} \underset{T \gg m_e}{\sim} \alpha^2 \left(\frac{T}{m} \right)^3 \left[\frac{4}{\pi^2} \left\{ \zeta(3) \frac{E}{m} \left[\left\{ 20 \left[1 + \frac{1}{v} \right] + 7v \right\} \ln \frac{1+v}{1-v} - \frac{4E}{m} \right] \right. \right.$$

$$\left. \left. + 2 \left[\frac{10m}{Ev} - \frac{E}{m} + \frac{7E}{mv} (1+v^2) \right] F_1 + \frac{\pi m}{6Ev} F_2 \right] \right],$$

Qader, M., Masood, S.S. and Ahmed, K. (1992) Physical Review D, 46, 5633.
<https://journals.aps.org/prd/abstract/10.1103/PhysRevD.46.5633>

Comparison of one and two-loop corrections at High T



Wavefunction Renormalization Constant

$$Z_2^{-1}(m\beta) = Z_2^{-1}(T=0) - \frac{2\alpha}{\pi} \int_0^\infty \frac{dk}{k} n_B(k) - \frac{3\alpha}{\pi} b(m\beta) \\ + \frac{\alpha T^2}{\pi v E^2} \ln \frac{1+v}{1-v} \left\{ \frac{\pi^2}{6} + m\beta a(m\beta) - c(m\beta) \right\},$$

Low T

$$Z_2^{-1} = Z_2^{-1}(T=0) - \frac{2\alpha}{\pi} \int \frac{dk}{k} n_B(k) - \frac{\alpha\pi T^2}{3E^2},$$

High T

$$Z_2^{-1} = Z_2^{-1}(T=0) - \frac{2\alpha}{\pi} \int \frac{dk}{k} n_B(k) - \frac{\alpha\pi T^2}{2E^2},$$



$$\begin{aligned}
Z_2^{-1} \xrightarrow{\Gamma \gg m} & 1 - \alpha \left[\frac{2I_A}{\pi} + \frac{1}{4\pi} \left(\frac{3}{\varepsilon} - 4 \right) + \frac{4\pi T^2}{3} \right] - \alpha^2 \left[\frac{1}{4\pi^3} \left\{ \frac{3}{\varepsilon} (I_A + J_A) + (3I_A + 5J_A) - \frac{8T^2}{3m^2} \right\} \right. \\
& + \frac{1}{8} \sum_{n,r,s=1}^{\infty} (-1)^r T \left\{ e^{-r\beta E} \left[f_+(s,r) \frac{\boldsymbol{\gamma} \cdot \mathbf{p}}{E^2 v^2} - \frac{I_B I_C}{64\pi^2} + h(p, \boldsymbol{\gamma}) \left\{ f_-(n,r) \frac{I_C}{8\pi} - f_-(s,r) \right\} + f_+(n,r) \frac{\boldsymbol{\gamma} \cdot \mathbf{p}}{E^2 v^2} \frac{I_B}{8\pi} \right. \right. \\
& \left. \left. + \left\{ \frac{2}{m} h(p, \boldsymbol{\gamma}) - \frac{\boldsymbol{\gamma} \cdot \mathbf{p}}{E^2 v^2} \right\} f_-(s,r) \right] \right\} \right].
\end{aligned}$$



Effect of Electron mass on different parameters

- Magnetic moment of electron
- Electromagnetic properties of particles that propagate in the presence of electron
- Effect on weak interaction processes (involving electrons) such as beta decay
- Decay rates and crosssections of particles



Electromagnetic vertex

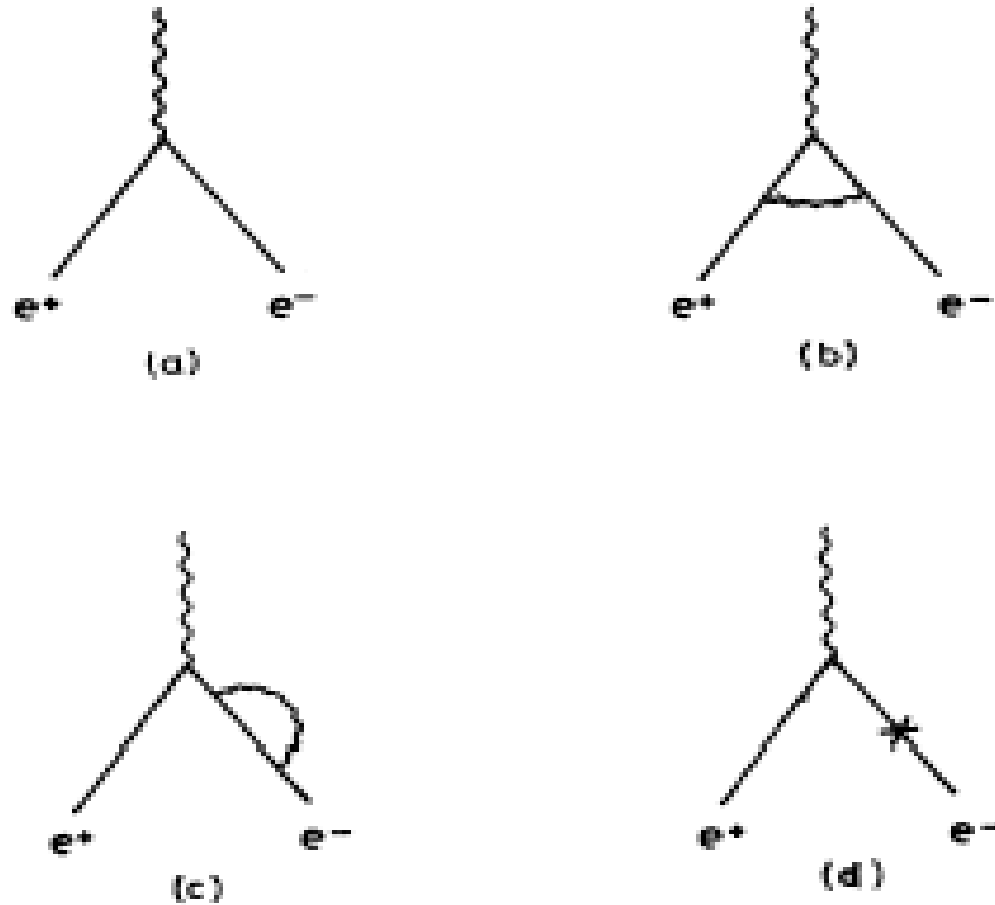


FIG. 3. The first-order radiative corrections to the electromagnetic vertex. (a) is the bare vertex, (b) the vertex corrections, (c) the self-energy correction to one of the legs, and (d) the mass counterterm insertion on one of the legs.

Z-Decay

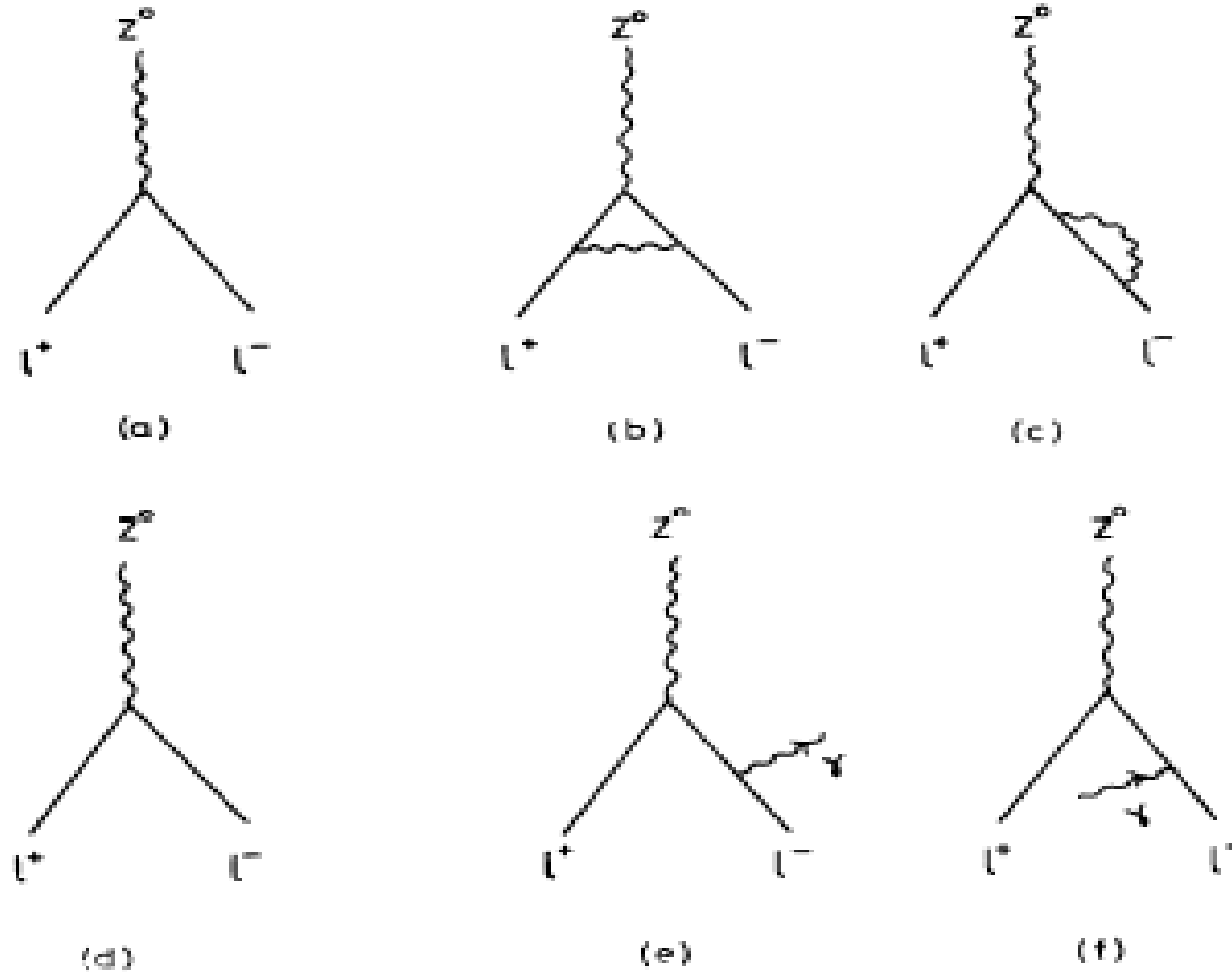


FIG. 1. The diagrams for the decay $Z^0 \rightarrow l^+ l^-$ up to the first order in α . (a) is the tree-level diagram, (b) is the vertex correction, (c) is the self-energy correction, (d) is the mass counter-term, (e) shows the bremsstrahlung emission and (f) the bremsstrahlung absorption.

Phase space contribution

$$\int \frac{d^3p}{(2\pi)^3} \frac{1}{2E_p} [1 - n_F(p \pm \mu)]$$

for fermions and

$$\int \frac{d^3k}{(2\pi)^3} \frac{1}{2E_k} [1 + n_B(k)]$$

$$\Delta\Gamma_{\text{ps}} = \frac{4\alpha}{\pi v^2} \left[\frac{9m_l^2}{m_Z^2} \bar{b}(m_l\beta, \mu) - \frac{6m_l T}{m_Z^2} \bar{a}(m_l\beta, \mu) - \frac{T^2}{m_Z^2} \left[1 - \frac{6}{\pi^2} \bar{c}(m_l\beta, \mu) \right] \right]. \quad (2.13)$$



Higgs Decay --- example

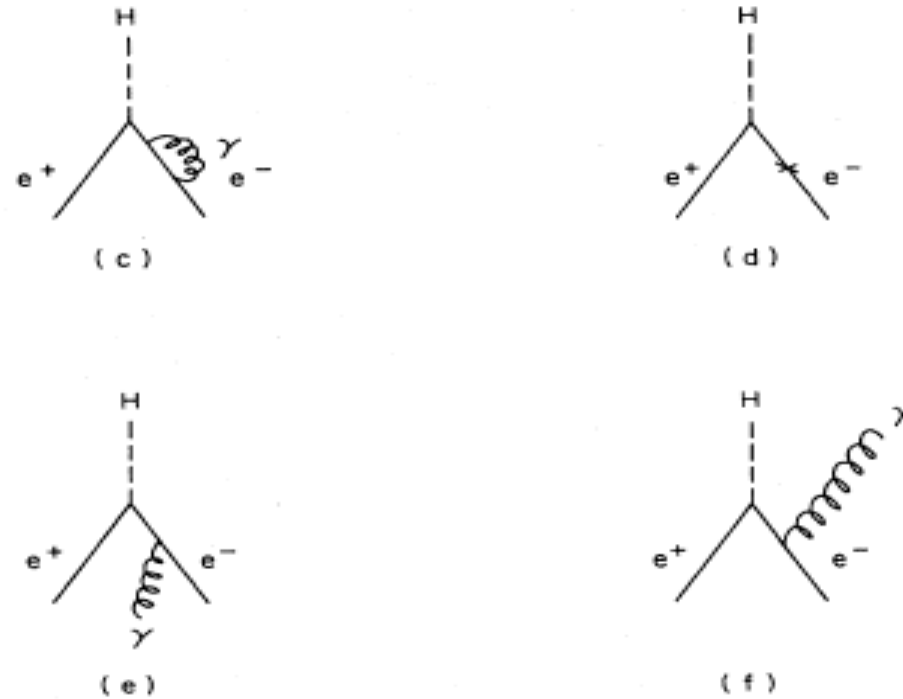


FIG. 2. Diagrams for $H \rightarrow e^+e^-$ to order α . Diagram (a) gives the bare coupling, (b) is the vertex correction, (c) and (d) are the self-energy and mass-counterterm contributions, respectively, while (e) and (f) correspond to real emission and absorption.



Taking the modulus squared and summing over spins

$$\sum_s |M|^2 = 4e^2 g^2 \left[(p_1 \cdot p_2 - m^2) \left[\frac{2p_1 \cdot p_2}{p_1 \cdot k p_2 \cdot k} - \frac{m^2}{(p_1 \cdot k)^2} - \frac{m^2}{(p_2 \cdot k)^2} \right] \right. \\ \left. + \left[2p_1 \cdot p_2 - m^2 \frac{p_1 \cdot k}{p_2 \cdot k} - m^2 \frac{p_2 \cdot k}{p_1 \cdot k} \right] \left[\frac{1}{p_1 \cdot k} + \frac{1}{p_2 \cdot k} \right] + \left[\frac{p_1 \cdot k}{p_2 \cdot k} + \frac{p_2 \cdot k}{p_1 \cdot k} + 2 \right] \right].$$

$$\Delta\Gamma_{\text{tot}} \simeq 2\Gamma_0 \left\{ \frac{\alpha T}{\pi E^2 v^2} \left[-m + \frac{1}{v} \left[m - \frac{1+v^2}{2} E \right] \ln \frac{1-v}{1+v} \right] a(m\beta) \right. \\ \left. + \frac{\alpha}{\pi v^2} \left[3v^2 - v \ln \frac{1-v}{1+v} + \frac{11}{2} \frac{m^2}{E^2} - \frac{1}{2} \right] b(m\beta) - \frac{\alpha T^2}{\pi E^2 v^3} \left[\ln \frac{1-v}{1+v} + 3v \right] c(m\beta) \right\}.$$



In order to calculate the contribution of stimulated emission or absorption from the heat bath, one must integrate (2.12) over the three-body phase space and carry out the Dalitz-plot analysis as done by DH. Since for bremsstrahlung, the relevant temperature correction accounts for the corresponding correction to the density of final states of photons: namely,

$$\frac{d^3p}{(2\pi)^3} \frac{1}{2E_p} [1 + n_B(E_p)] ; \quad (2.13)$$

therefore, no modification is expected in this case in the DH results. We shall return to this question in the next subsection dealing with the decay rate of $H \rightarrow e^+ e^-$.

$$\begin{aligned} \Delta\Gamma_{\text{FS}} \simeq & 36 \frac{\alpha}{\pi v^2} \frac{m^*}{m_H^2} b(m\beta) - 24 \frac{\alpha}{\pi v^2} \frac{mI}{m_H^2} a(m\beta) \\ & - \frac{4\alpha\pi}{v^2} \frac{T^2}{m_H^2} \left[1 - \frac{6}{\pi^2} c(m\beta) \right] + O(T^4). \end{aligned}$$



$$\Delta\Gamma_{\text{tot}} \simeq \frac{4\alpha\Gamma_0}{\pi} \left\{ \frac{T}{m_Z v} \left[\left[1 - \frac{2m_l}{m_Z} + \frac{4m_l^2}{m_Z^2 v^2} \right] \ln \frac{1+v}{1-v} - \frac{2m_l}{m_Z v} \left[3 + \frac{4m_l}{m_Z^2 v^3} \right] \right] \right. \\
\times \bar{a}(m_l\beta, \mu) + \left[1 + \frac{2m_l^2}{m_Z^2 v^2} - \frac{1}{2v} \left[1 - \frac{5}{4} \frac{m_l^2}{m_Z^2 v^2} + \frac{m_l^2}{4m_Z^2 v^4} \right] \ln \frac{1+v}{1-v} \right] \\
\left. \times \tilde{b}(m_l\beta, \mu) + \frac{2T^2}{m_Z^2 v} \left[\left[1 + \frac{m_l^2}{m_Z^2 v^3} \right] \ln \frac{1+v}{1-v} + \frac{1}{v} \left[3 - \frac{2m_l^2}{m_Z^2 v^2} \right] \right] \tilde{c}(m_l\beta, \mu) \right\}$$

$$\bar{a}(m_l\beta, \mu) = \frac{1}{2} \ln \left[\left[1 + e^{-(m_l - \mu)\beta} \right] \left[1 + e^{-(m_l + \mu)\beta} \right] \right]$$

$$\tilde{b}(m_l\beta, \mu) = \sum_{n=1}^{\infty} (-1)^n \cosh(n\beta\mu) \text{Ei}(-nm_l\beta),$$

$$\tilde{c}(m_l\beta, \mu) = \sum_{n=1}^{\infty} (-1)^n \cosh(n\beta\mu) \frac{e^{-nm_l\beta}}{n^2}.$$

$$\Delta\Gamma_{\text{tot}} \xrightarrow{T > m_e} -\frac{2\pi\alpha\Gamma_0}{3} \frac{T^2}{m_Z^2 v^3} \left[\left[1 + \frac{m_l^2}{m_Z^2 v^3} \right] \ln \frac{1+v}{1-v} + \frac{1}{v} \left[3 - \frac{2m_l^2}{m_Z^2 v^2} \right] \right]$$



TABLE II. Temperature corrections to the decay rate of $H \rightarrow e^+e^-$ are computed for different values of temperature at $m_H = 1 \text{ GeV}/c^2$. The table shows that these corrections become significant for certain temperatures.

| $m\beta$ | T (MeV and K) | $\Delta\Gamma_{\text{tot}}/\Gamma_0$ | Percentage change in the decay rate |
|----------|---------------------------|--------------------------------------|--|
| 0.001 | $500/5.93 \times 10^{12}$ | 0.2629 | 26.29 |
| 0.005 | $100/1.19 \times 10^{12}$ | 0.2275 | 22.75 |
| 0.01 | $50/5.93 \times 10^{11}$ | 0.1834 | 18.34 |
| 0.05 | $10/1.19 \times 10^{11}$ | 0.1147 | 11.47 |
| 0.10 | $5/5.93 \times 10^{10}$ | 0.0843 | 8.43 |
| 0.5 | $1/1.19 \times 10^{10}$ | 0.0326 | 3.26 |
| 1.0 | $0.5/5.93 \times 10^9$ | 0.0147 | 1.47 |
| 2.0 | $0.25/2.96 \times 10^9$ | 0.0037 | 0.37 |



Lamb Shift

The Lamb shift is a purely measurable perturbative effect, which causes a small change in wavelength. Knight has looked at the thermal effects on the Lamb shift. A small shift in the bound state energies is calculated from the regular quantum mechanical energy values corresponding to the integral values on n such that:

$$E_n = -\frac{me^4}{8(nh\epsilon_0)^2}$$

$$E = E_f - E_i = \left(\frac{me^4}{8(nh\epsilon_0)^2}\right)\left(\frac{1}{n_i^2} - \frac{1}{n_f^2}\right)$$

The change in the electron mass will affect the energies of the energy levels. Comparing these formulae with the Rydberg formula gives a shift on energy between successive energy levels as

$$R_H = -\frac{me^4}{8h^3\epsilon_0^2}$$

On the other hand the total energy shift due to the vacuum polarization is determined as:

$$\Delta E = \int d^3r \Delta V(r)|\psi(r)|^2$$

1. P.L.Knight, J. Phys. A: Gen. Phys., Vol. 5, March (1972.), 'Effects of External Fields on the Lamb Shift' (417-425)



$$\Delta V(r) = \frac{e^2}{(2\pi)^3} \int d^3q e^{iq \cdot r} \left[\frac{\tilde{\Pi}(q)}{q^2} \right]$$

$$\Delta E_n = \frac{-4\alpha^5 m}{15\pi n^3}$$

n is the Landau number and is associated with the Landau levels of energy for the Fermi gas of electron. This correction may not be relevant for atoms for temperature dependent electron mass as the existence of atoms is not expected at 10^{10} K. However, high chemical potential is not necessarily ignorable for large molecules.



Lecture 2

- Light is the major source of information for astronomical observations.
- Properties of light can be related to the properties of their source.
- Information of the source can help to understand the origin of the radiation
- It may provide a little more information about the structure and composition of the source of radiation.
- The nature of the wave can help to determine the collective properties of the medium as well.



Renormalization of Photon Propagator

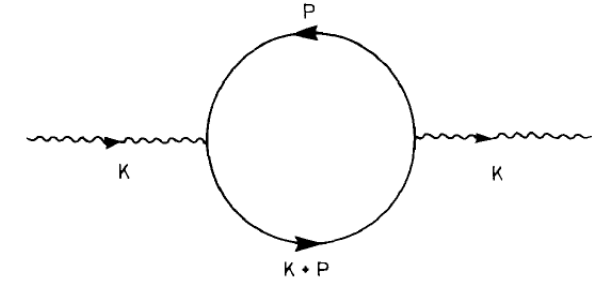
$$D'_{\mu\nu}(k) = \text{diagram 1} + \text{diagram 2} + \text{diagram 3} + \dots$$
$$= \frac{1}{D^{-1}_{\mu\nu} - i\Pi_{\mu\nu}} = \frac{-i}{k^2 - \mathcal{O}(\Lambda^2)} \left(g_{\mu\nu} - \frac{k_\mu k_\nu}{k^2} \right)$$

The diagrams represent the perturbative expansion of the photon propagator. The first diagram is a simple wavy line with indices μ and ν and momentum k . The second diagram is a wavy line with a fermion loop (circle) with momenta p and $p+k$. The third diagram is a wavy line with two fermion loops in series, each with momenta p and $p+k$.



Calculation of Charge Renormalization

$$\pi_{\mu\nu}(K, \mu) = ie^2 \int \frac{d^4 p}{(4\pi)^4} \text{Tr} \{ \gamma_\mu(\not{p} + \not{K} + m) \gamma_\nu(\not{p} + m) \} \left[\frac{1}{(p+K)^2 - m^2} + \Gamma_F(p+K, \mu) \right] \left[\frac{1}{p^2 - m^2} + \Gamma_F(p, \mu) \right],$$

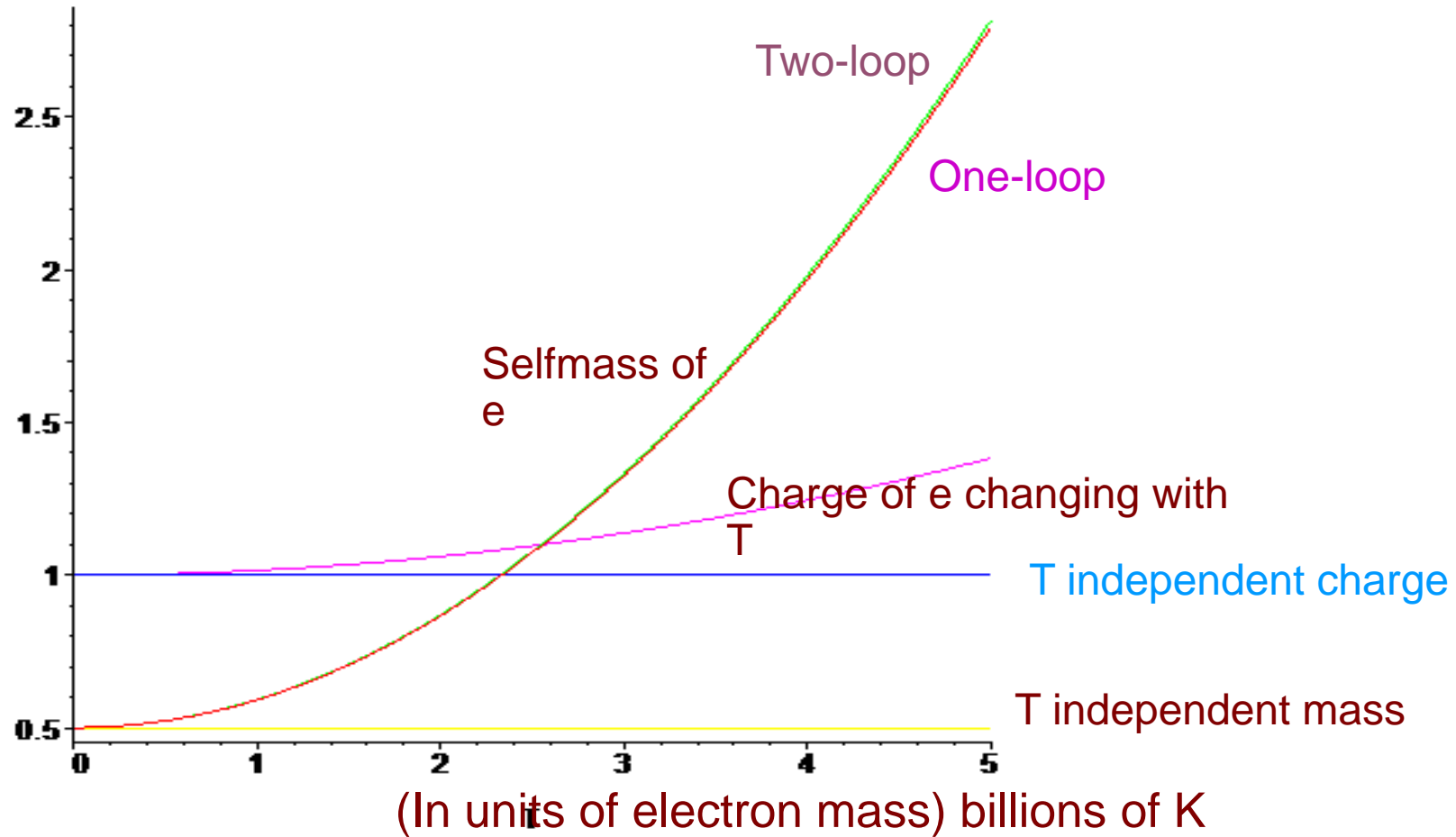


$$\Gamma_F(p, \mu) = 2\pi i \delta(p^2 - m^2) [\theta(p_0) n_F(p, \mu) + \theta(-p_0) n_F(p, -\mu)]$$

$$\pi_{\mu\nu}^\beta(K, \mu) = -\frac{2\pi e^2}{2} \int \frac{d^4 p}{(2\pi)^4} \text{Tr} \{ \gamma_\mu(\not{p} + \not{K} + m) \gamma_\nu(\not{p} + m) \} \times \left[\frac{\delta[(p+K)^2 - m^2]}{p^2 - m^2} \{ n_F(p+K, \mu) + n_F(p+K, -\mu) \} + \frac{\delta(p^2 - m^2)}{(p+K)^2 - m^2} \{ n_F(p, \mu) + n_F(p, -\mu) \} \right].$$



Thermal Corrections



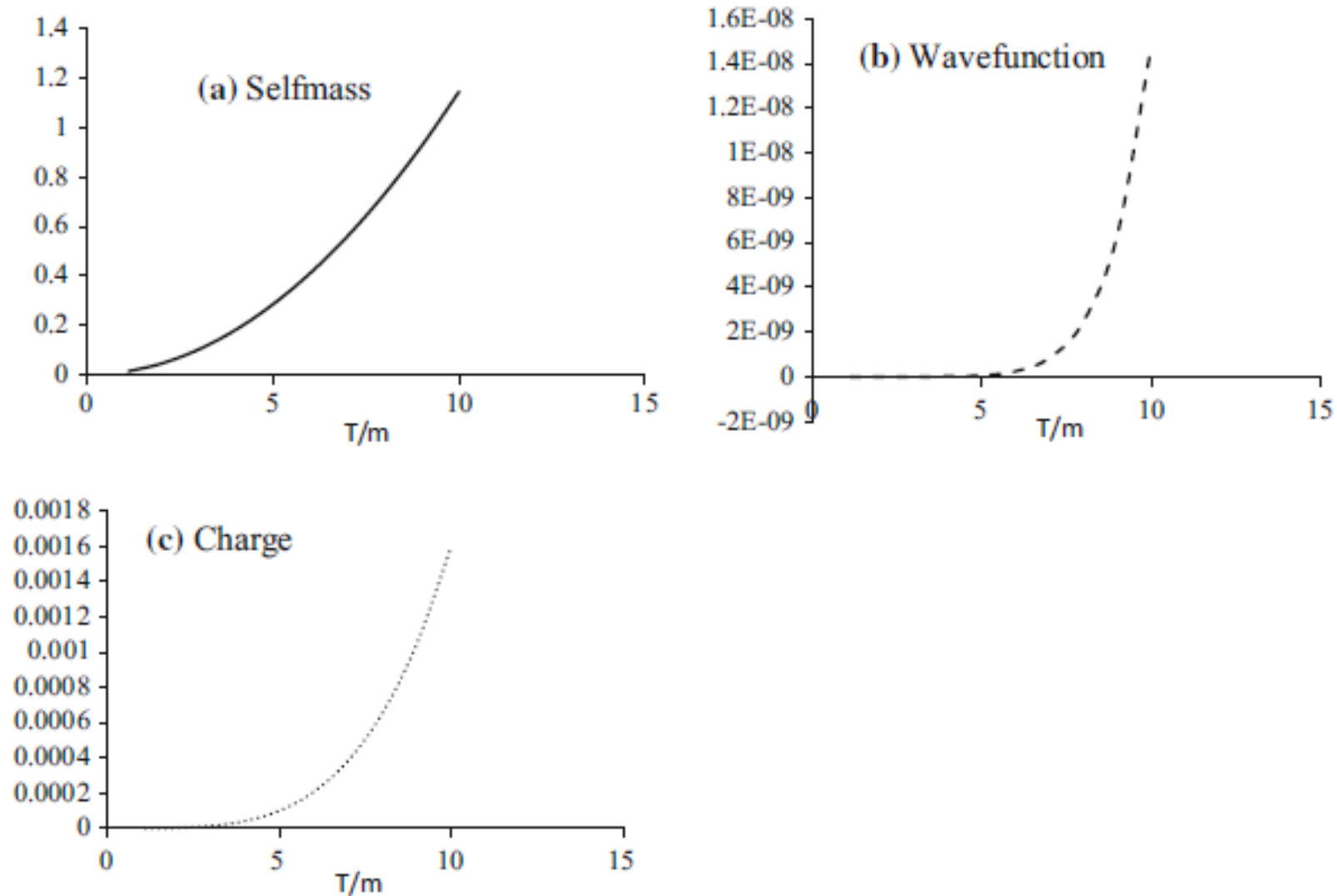
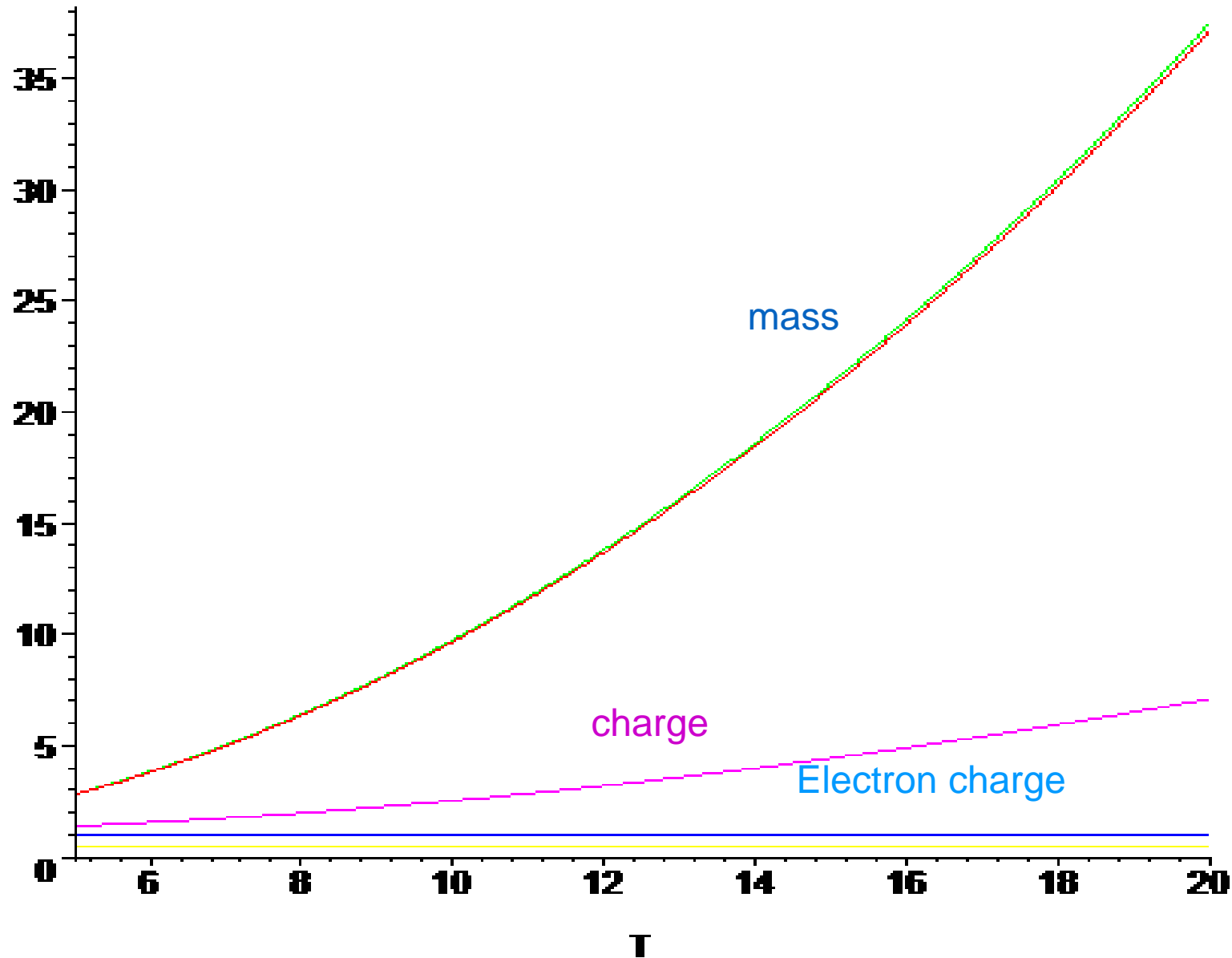


Fig. 2 The properties of the electrons as a function of temperature (in units of m). The thermal corrections to **a** electron mass; **b** wave function; and **c** charge

Masood, S.S. Eur. Phys. J. C (2017) 77: 826. <https://doi.org/10.1140/epjc/s10052-017-5398-0> .



ELECTRON MASS and CHARGE at High T



Electron mass



$$\pi_L(k, \omega) = -\frac{K^2}{k^2} u^\mu u^\nu \pi_{\mu\nu}$$

$$\pi_T(k, \omega) = -\frac{1}{2}\pi_L + \frac{1}{2}g^{\mu\nu}\pi_{\mu\nu}.$$

$$c(m\beta) \xrightarrow{m\beta \ll 1} -\frac{\pi^2}{12},$$

$$\pi_L \simeq \frac{e^2 T^2}{3} \left(1 - \frac{\omega^2}{k^2}\right) \left[1 - \frac{\omega}{2k} \ln \frac{\omega + k}{\omega - k}\right]$$

$$\pi_T \simeq \frac{e^2 T^2}{6} \left[\frac{\omega^2}{k^2} + \left(1 - \frac{\omega^2}{k^2}\right) (\omega/2k) \ln \frac{\omega + k}{\omega - k} \right],$$

.K.Ahmed and Samina Saleem, Ann.Phys.164, (1991) 460.



$$\pi_{\mu\nu}(K) = \pi_{\text{T}}(k, \omega) P_{\mu\nu} + \pi_{\text{L}}(k, \omega) Q_{\mu\nu}.$$

$$P_{\mu\nu} = \tilde{g}_{\mu\nu} + \tilde{K}_{\mu} \tilde{K}_{\nu} / k^2$$

$$\tilde{g}_{\mu\nu} = g_{\mu\nu} - u_{\mu} u_{\nu}$$

$$\tilde{K}_{\mu} = K_{\mu} - \omega u_{\mu}$$

$$Q_{\mu\nu} = -\frac{1}{k^2 K^2} (k^2 u_{\mu} + \omega \tilde{K}_{\mu})(k^2 u_{\nu} + \omega \tilde{K}_{\nu}),$$

$$P_{\nu}^{\mu} P_{\alpha}^{\nu} = P_{\alpha}^{\mu}, \quad Q_{\alpha}^{\mu} = Q_{\nu}^{\mu} Q_{\alpha}^{\nu},$$

$$K_{\mu} P_{\nu}^{\mu} = 0, \quad K_{\mu} Q_{\nu}^{\mu} = 0.$$



$$\pi_{\mu\nu} = \begin{pmatrix} -\frac{k^2}{K^2} \pi_L & -\frac{i\omega k_1}{K^2} \pi_L & -\frac{i\omega k_2}{K^2} \pi_L & -\frac{i\omega k_3}{K^2} \pi_L \\ -\frac{i\omega k_1}{K^2} \pi_L & \left(-1 - \frac{k_1^2}{k^2}\right) \pi_T + \left(\frac{\omega^2 k_1^2}{k^2 K^2}\right) \pi_L & \left(-\frac{k_1 k_2}{k^2}\right) \pi_T + \left(\frac{\omega^2 k_1 k_2}{k^2 K^2}\right) \pi_L & \left(-\frac{k_1 k_3}{k^2}\right) \pi_T + \left(\frac{\omega^2 k_1 k_3}{k^2 K^2}\right) \pi_L \\ -\frac{i\omega k_2}{K^2} \pi_L & \left(-\frac{k_1 k_2}{k^2}\right) \pi_T + \left(\frac{\omega^2 k_1 k_2}{k^2 K^2}\right) \pi_L & \left(-1 - \frac{k_2^2}{k^2}\right) \pi_T + \left(\frac{\omega^2 k_2^2}{k^2 K^2}\right) \pi_L & \left(-\frac{k_2 k_3}{k^2}\right) \pi_T + \left(\frac{\omega^2 k_2 k_3}{k^2 K^2}\right) \pi_L \\ -\frac{i\omega k_3}{K^2} \pi_L & \left(-\frac{k_1 k_3}{k^2}\right) \pi_T + \left(\frac{\omega^2 k_1 k_3}{k^2 K^2}\right) \pi_L & \left(-\frac{k_2 k_3}{k^2}\right) \pi_T + \left(\frac{\omega^2 k_2 k_3}{k^2 K^2}\right) \pi_L & \left(-1 - \frac{k_3^2}{k^2}\right) \pi_T + \left(\frac{\omega^2 k_3^2}{k^2 K^2}\right) \pi_L \end{pmatrix}.$$



$$P_{\mu\nu} = \begin{pmatrix} 0 & 0 & 0 & 0 \\ 0 & -1 - \frac{k_1^2}{k^2} & -\frac{k_1 k_2}{k^2} & -\frac{k_1 k_3}{k^2} \\ 0 & -\frac{k_1 k_2}{k^2} & -1 - \frac{k_2^2}{k^2} & -\frac{k_2 k_3}{k^2} \\ 0 & -\frac{k_1 k_3}{k^2} & -\frac{k_2 k_3}{k^2} & -1 - \frac{k_3^2}{k^2} \end{pmatrix}$$

$$Q_{\mu\nu} = \begin{pmatrix} -\frac{k^2}{K^2} & -\frac{i\omega k_1}{K^2} & -\frac{i\omega k_2}{K^2} & -\frac{i\omega k_3}{K^2} \\ -\frac{i\omega k_1}{K^2} & \frac{\omega^2 k_1^2}{k^2 K^2} & \frac{\omega^2 k_1 k_2}{k^2 K^2} & \frac{\omega^2 k_1 k_3}{k^2 K^2} \\ -\frac{i\omega k_2}{K^2} & \frac{\omega^2 k_1 k_2}{k^2 K^2} & \frac{\omega^2 k_2^2}{k^2 K^2} & \frac{\omega^2 k_2 k_3}{k^2 K^2} \\ -\frac{i\omega k_3}{K^2} & \frac{\omega^2 k_1 k_3}{k^2 K^2} & \frac{\omega^2 k_2 k_3}{k^2 K^2} & \frac{\omega^2 k_3^2}{k^2 K^2} \end{pmatrix},$$



$$\pi_L \simeq \frac{4e^2}{\pi^2} \left(1 - \frac{\omega^2}{k^2}\right) \left[\left(1 - \frac{\omega}{2k} \ln \frac{\omega+k}{\omega-k}\right) \left(\frac{m\tilde{a}(m\beta, \mu)}{\beta} - \frac{\tilde{c}(m\beta, \mu)}{\beta^2}\right) + \frac{1}{4} \left(2m^2 - \omega^2 + \frac{11k^2 + 37\omega^2}{72}\right) \tilde{b}(m\beta, \mu) \right]$$

$$\pi_T \simeq \frac{2e^2}{\pi^2} \left[\left\{ \frac{\omega^2}{k^2} + \left(1 - \frac{\omega^2}{k^2}\right) \ln \frac{\omega+k}{\omega-k} \right\} \left(\frac{m\tilde{a}(m\beta, \mu)}{\beta} - \frac{\tilde{c}(m\beta, \mu)}{\beta^2}\right) + \frac{1}{8} \left\{ 2m^2 + \omega^2 + \frac{107\omega^2 - 131k^2}{72} \right\} \tilde{b}(m\beta, \mu) \right],$$

$$\tilde{a}(m\beta, \mu) = \frac{1}{2} \ln \{ (1 + e^{-\beta(m+\mu)})(1 + e^{-\beta(m-\mu)}) \}$$

$$\tilde{b}(m\beta, \mu) = \sum_{n=1}^{\infty} (-1)^n \cosh(n\beta\mu) Ei(-nm\beta)$$

$$Ei(-x) = - \int_x^{\infty} \frac{e^{-t}}{t} dt.$$

$$\tilde{c}(m\beta, \mu) = \sum_{n=1}^{\infty} (-1)^n \frac{e^{-nm\beta}}{n^2} \cosh(n\beta\mu)$$



Charge Renormalization Constant

$$Z_3 \cong 1 + \frac{2e^2}{\pi^2} \left[\frac{ma(m\beta, \mu)}{\beta} - \frac{c(m\beta, \mu)}{\beta^2} + \frac{1}{4} \left(m^2 + \frac{1}{3}\omega^2 \right) b(m\beta, \mu) \right].$$



Dynamically Generated Mass of Photon

$$K_\mu(\omega, \mathbf{k}) \rightarrow 0, \quad K_0 = \omega = 0 \quad ;$$

$$\lim_{\mathbf{k} \rightarrow 0} \pi_L(0, \mathbf{k}) \equiv K_L^2 = \frac{4e^2}{\pi^2} \left[\frac{m\tilde{a}(m\beta, \mu)}{\beta} - \frac{\tilde{c}(m\beta, \mu)}{\beta^2} + \frac{m^2}{2} \cdot \tilde{b}(m\beta, \mu) \right]$$

$$\lim_{\mathbf{k} \rightarrow 0} \pi_T(0, \mathbf{k}) \equiv K_T^2 = 0.$$



Plasma Screening Mass

$$\lambda_D = \Pi_L.$$

$$\lambda_D = \left(\frac{\varepsilon k_B T}{\sum_{j=1}^N n_j^0 q_j^2} \right)^{1/2}.$$

$$v_{\text{prop}} = \sqrt{\frac{1}{\mu(K)\varepsilon(K)}},$$

$$\omega_D = \frac{2\pi v_{\text{prop}}}{\lambda_D} = 2\pi K_L v_{\text{prop}},$$

$$r_i = \frac{c}{v_{\text{prop}}} = \sqrt{\frac{\mu(K)\varepsilon(K)}{\mu_0(K)\varepsilon_0(K)}}.$$



: if we set $\omega = |\mathbf{k}| = k$ with $k \rightarrow 0$ then

$$\lim_{k \rightarrow 0} \pi_{\text{T}}(k, \mathbf{k}) \equiv \omega_{\text{T}}^2 = \frac{2e^2}{\pi^2} \left[\frac{m\tilde{a}(m\beta, \mu)}{\beta} - \frac{\tilde{c}(m\beta, \mu)}{\beta^2} + \frac{m^2}{4} \tilde{b}(m\beta, \mu) \right]$$

$$\lim_{\mathbf{k} \rightarrow 0} \pi_{\text{L}}(|\mathbf{k}|, \mathbf{k}) \equiv \omega_{\text{L}}^2 = 0.$$

$$\omega_{\text{T}}^2 = \frac{2e^2}{\pi^2} \left[\frac{m\tilde{a}}{\beta} - \frac{\tilde{c}}{\beta^2} + \frac{m^2}{4} \tilde{b} \right]$$



At very high T

$$D'_{F\mu\nu} = \frac{P_{\mu\nu}}{K^2 - \pi_T} + \frac{Q_{\mu\nu}}{K^2 - \pi_L}.$$

$$\omega_T^2 \xrightarrow{m\beta \rightarrow 0} \frac{2e^2}{\pi^2} (-1/\beta^2) \lim_{m\beta \rightarrow 0} c(m\beta) = \frac{2e^2}{\pi^2} (-1/\beta^2) \left(\frac{-\pi^2}{12} \right) = \frac{e^2 T^2}{6}.$$

$$K_L^2 \xrightarrow[\mu=0]{m\beta \rightarrow 0} -\frac{4e^2}{\pi^2} \frac{c(0,0)}{\beta^2} = \frac{e^2 T^2}{3}.$$



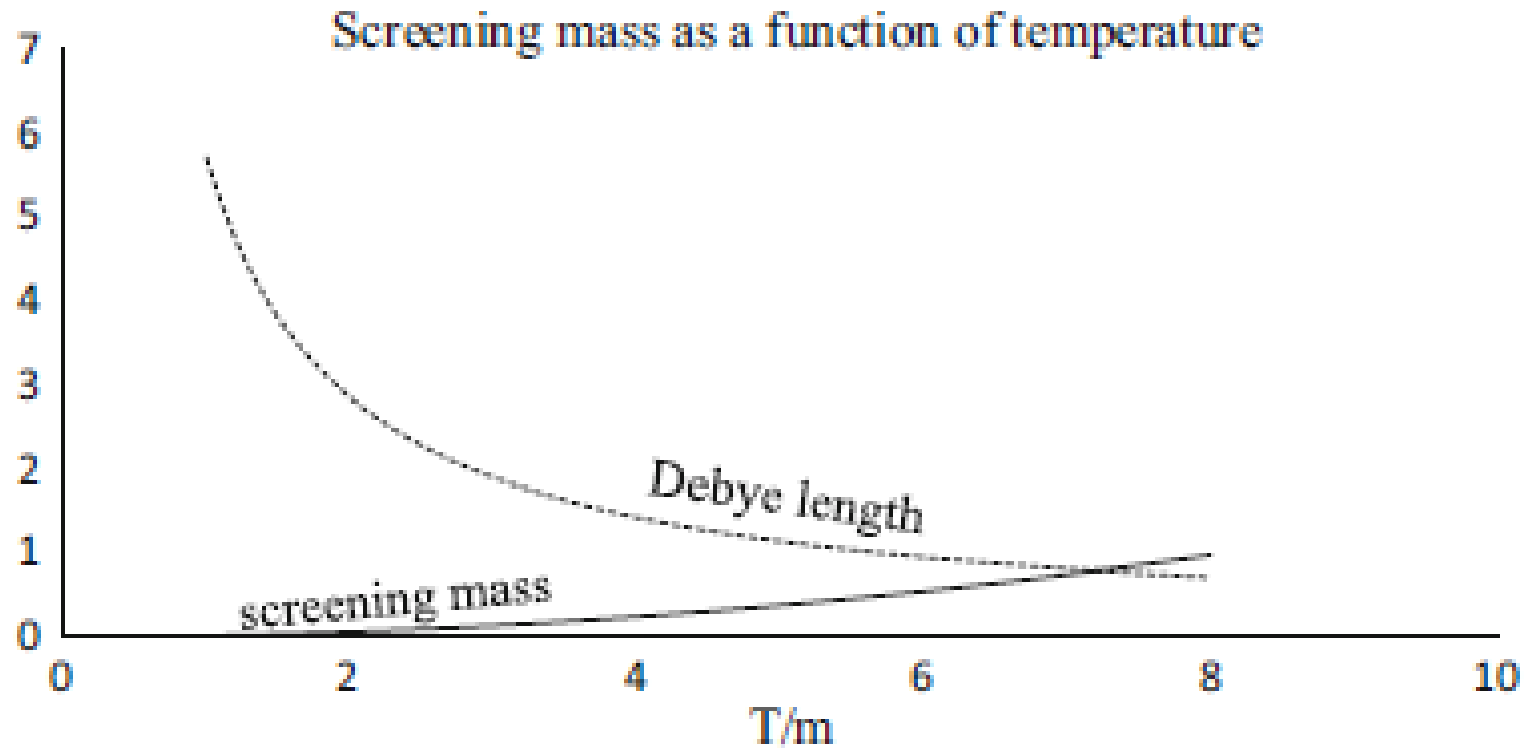
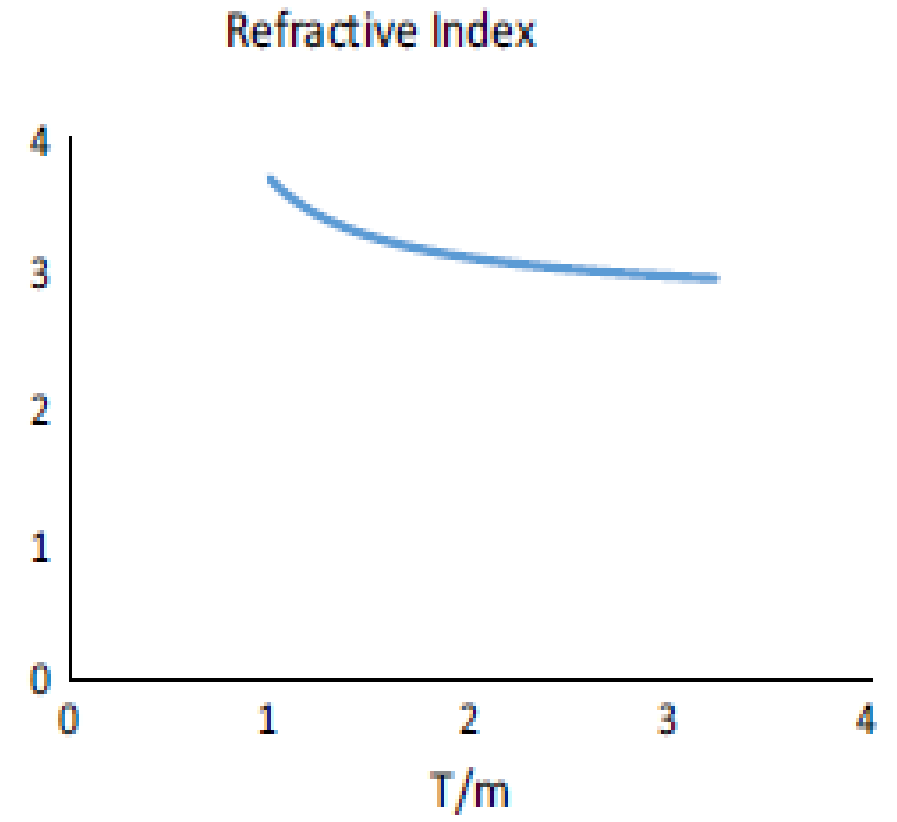
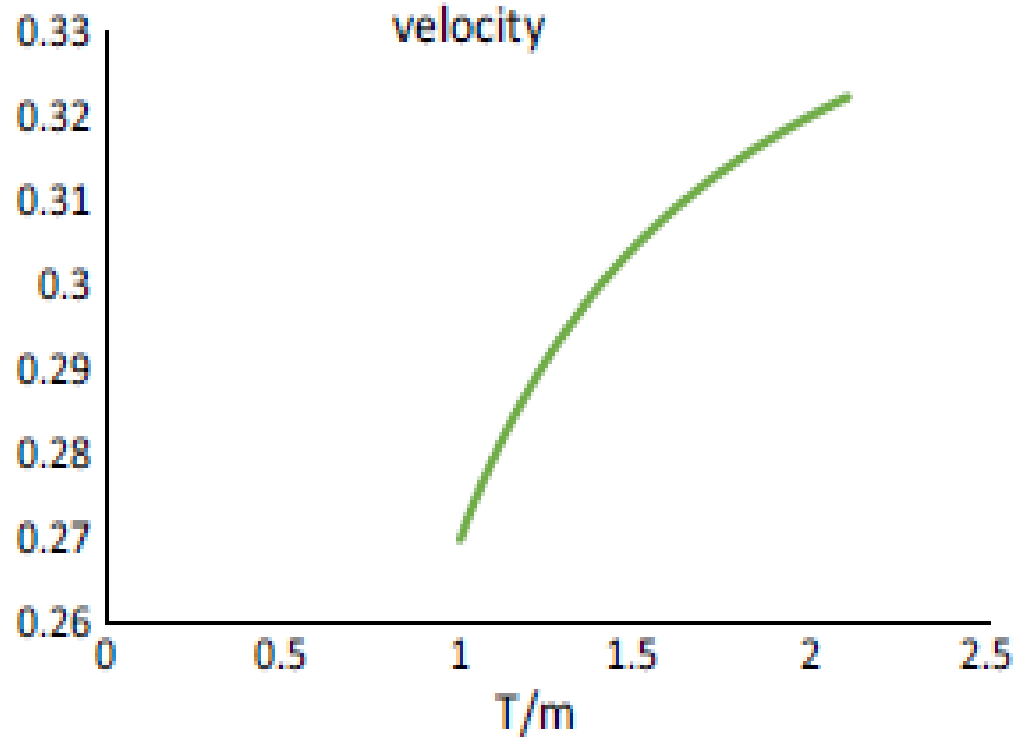


Fig. 5 Plot of plasma screening mass (solid line) and the corresponding Debye shielding length (broken line) as a function of temperature in units of the electron mass





Electromagnetic Properties

Electric Permittivity

$$\varepsilon(k) = 1 - \frac{\pi_L(K)}{k^2},$$

Magnetic Permeability

$$\frac{1}{\mu(k)} = \frac{k^2 \pi_T(K) - \omega^2 \pi_L(K)}{k^2 K^2},$$

Speed

Refractive Index

$$\varepsilon(K) = 1 + \chi_e$$

$$\mu(K) = 1 + \chi_m$$

$$v_{\text{prop}} = \sqrt{\frac{1}{\varepsilon(K)\mu(K)}},$$

$$r_i = \frac{c}{v} = \sqrt{\frac{\varepsilon(K)\mu(K)}{\varepsilon_0(K)\mu_0(K)}}.$$

χ_e and χ_m give the dielectric constant and magnetization of a medium



(1) For $\mu \gg T$ and $\omega \gg m \gg k$, we obtain from the above equations

$$\varepsilon_E(k, \mu) = 1 + \frac{2\alpha}{\pi^2} \left[\frac{\mu^2}{4k^2} + \frac{2m^2\omega^2}{k^4} \ln \frac{\mu}{m} \right],$$

$$\frac{1}{\mu_B(k, \mu)} = 1 + \frac{2\alpha}{\pi} \frac{\omega^6}{k^6} \left[\frac{3}{16} \frac{k^2}{4m^2} - \frac{2m^2}{\omega^2} \ln \frac{\mu}{m} \right].$$

(2) For $\mu \gg T$ and $\omega \ll m \ll k$,

$$\varepsilon_E(k, \mu) = 1 + \frac{\alpha}{2\pi^2} \left[\frac{\mu^2}{k^2} + \frac{11}{48} \frac{k^2}{m^2} \right],$$

$$\frac{1}{\mu_B(k, \mu, T)} = 1 + \frac{\alpha}{2\pi} \left[\frac{3}{32} \frac{k^2}{m^2} \right].$$



$$\varepsilon(K) \cong 1 - \frac{4e^2}{\pi^2 K^2} \left(1 - \frac{\omega^2}{\mathbf{k}^2}\right) \left\{ \left(1 - \frac{\omega}{2\mathbf{k}} \ln \frac{\omega + \mathbf{k}}{\omega - \mathbf{k}}\right) \left(\frac{ma(m\beta, \mu)}{\beta} - \frac{c(m\beta, \mu)}{\beta^2}\right) + \frac{1}{4} \left(2m^2 - \omega^2 + \frac{11k^2 + 37\omega^2}{72}\right) b(m\beta, \mu) \right\},$$

$$\frac{1}{\mu(K)} \cong 1 - \frac{2e^2}{\pi^2 k^2 K^2} \left[\omega^2 \left\{ \left(1 - \frac{\omega^2}{\mathbf{k}^4} - \left(1 + \frac{\mathbf{k}^2}{\omega^2}\right) \left(1 - \frac{\omega^2}{\mathbf{k}^2}\right) \frac{\omega}{2\mathbf{k}} \ln \frac{\omega + \mathbf{k}}{\omega - \mathbf{k}} \right\} \times \left(\frac{ma(m\beta, \mu)}{\beta} - \frac{c(m\beta, \mu)}{\beta^2}\right) - \frac{1}{8} \left(6m^2 - \omega^2 + \frac{129\omega^2 - 109k^2}{72}\right) b(m\beta, \mu) \right\} \right].$$



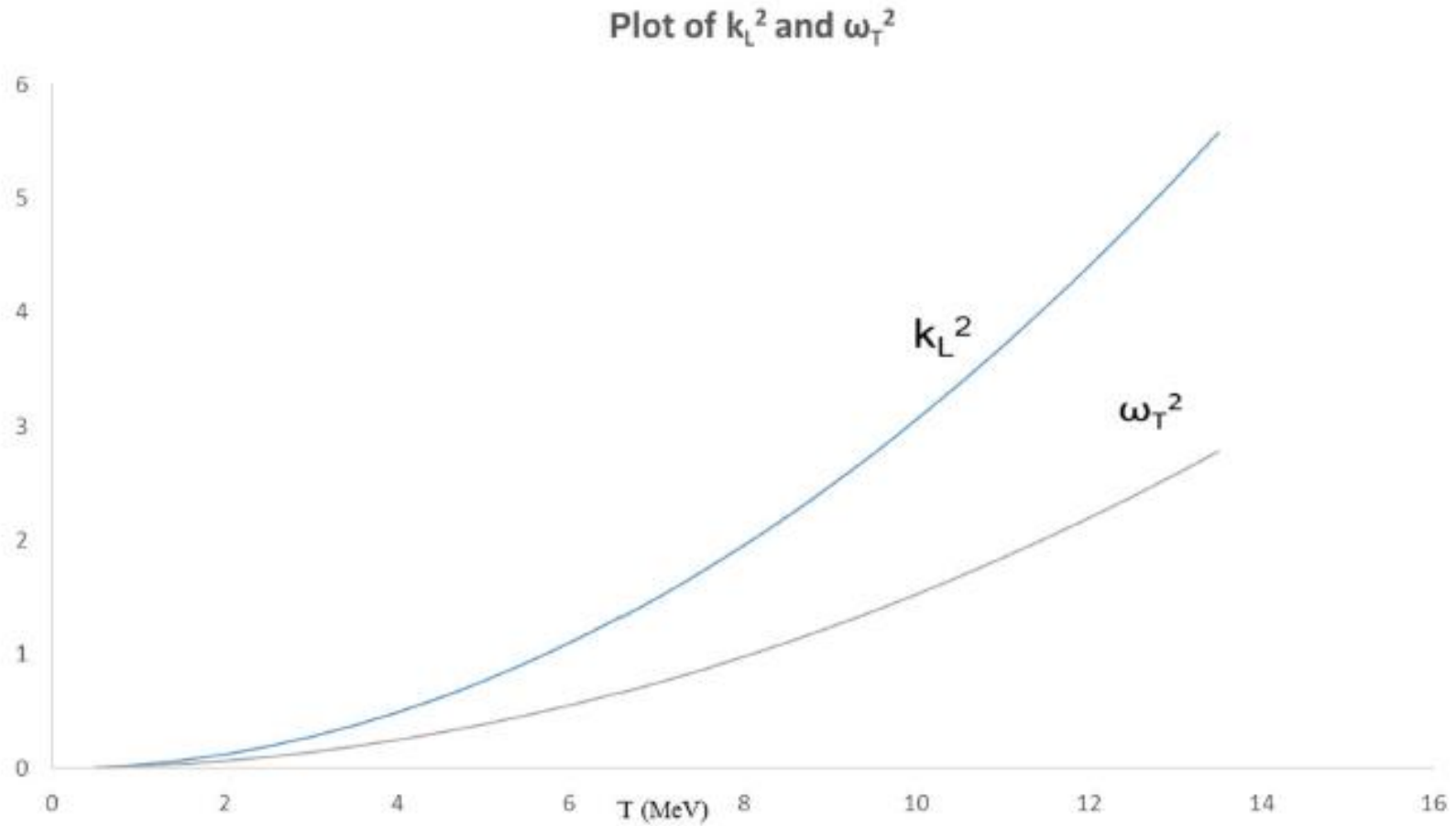


Fig. 1 Temperature dependence of the longitudinal component of the propagation vector (square) and the transverse frequency (square) is plotted showing that the Debye shielding length is greater than the plasma frequency



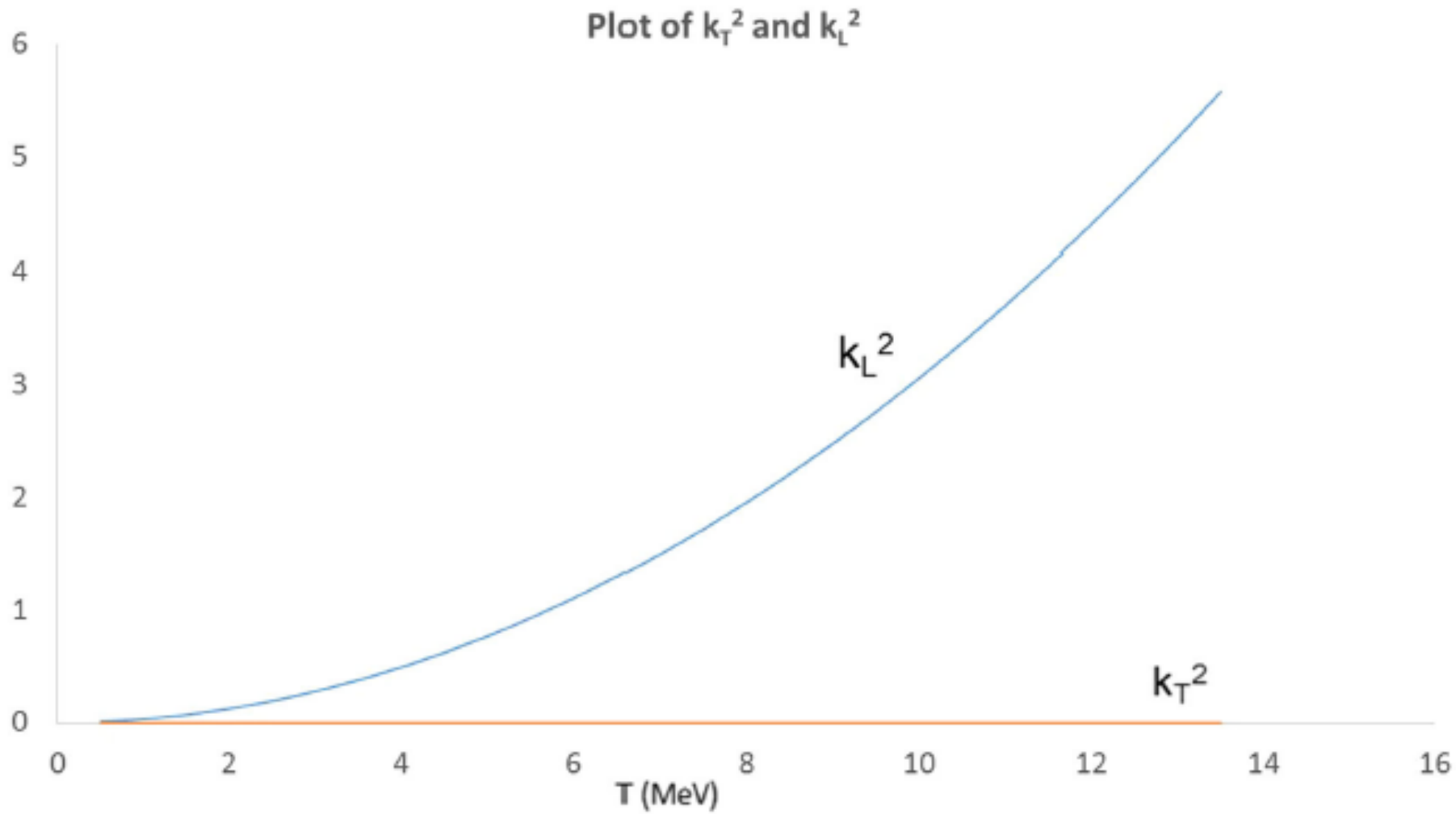


Fig. 2 On comparing the plots of K_L^2 and K_T^2 , it can be clearly seen that the propagation vector in the transverse direction is independent of temperature. The inverse of Debye length ($1/k_L$) increases with temperature, but the transverse motion will not be affected



Plot of Plasma Frequency and Debye Length

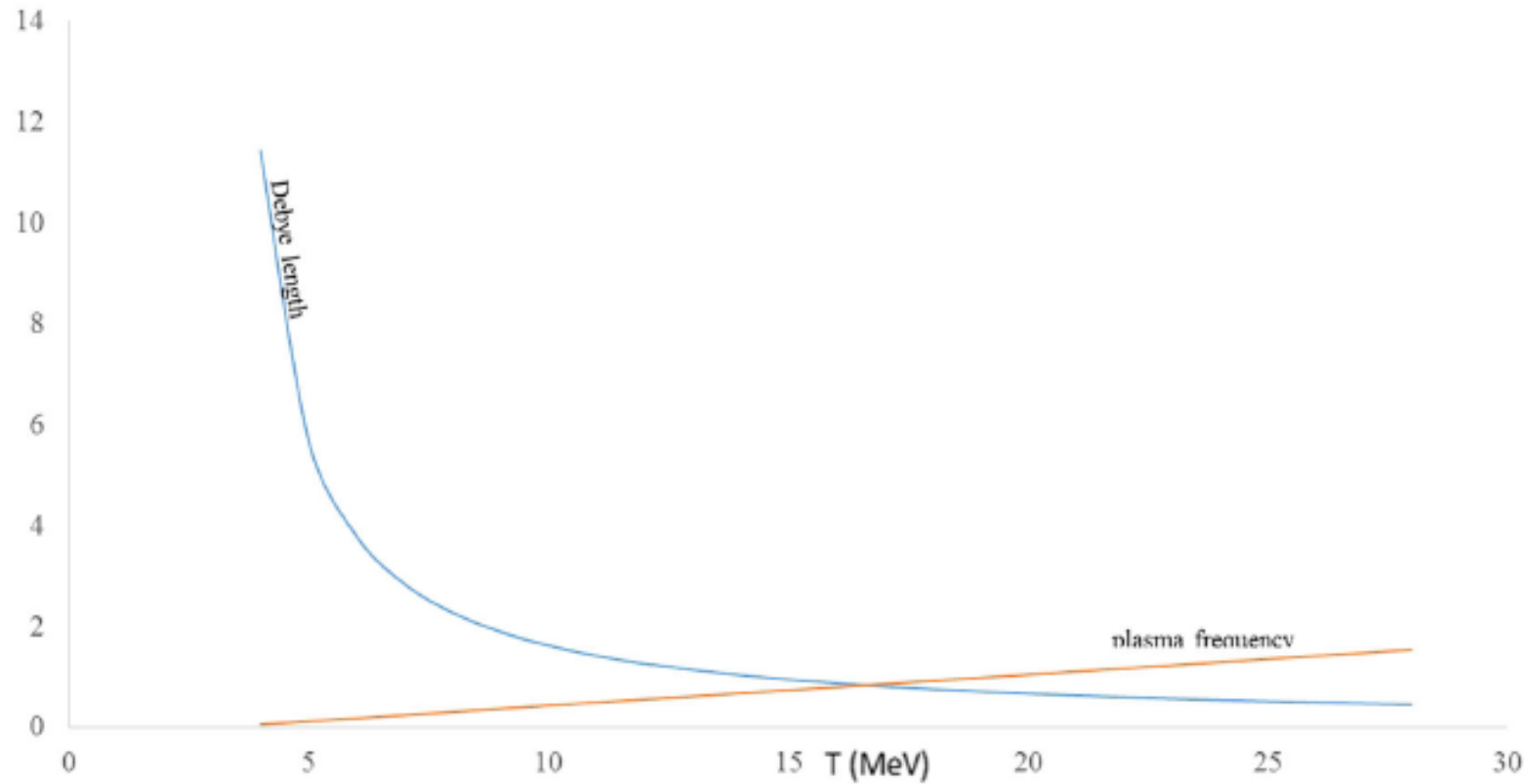


Fig. 4 Debye length and the plasma frequency are plotted as a function of temperature showing that the screening length increases with T . When temperature rises around 16 times the mass of the electron which is around 8 MeV, a phase transition takes place and the plasma frequency becomes greater than the shielding length



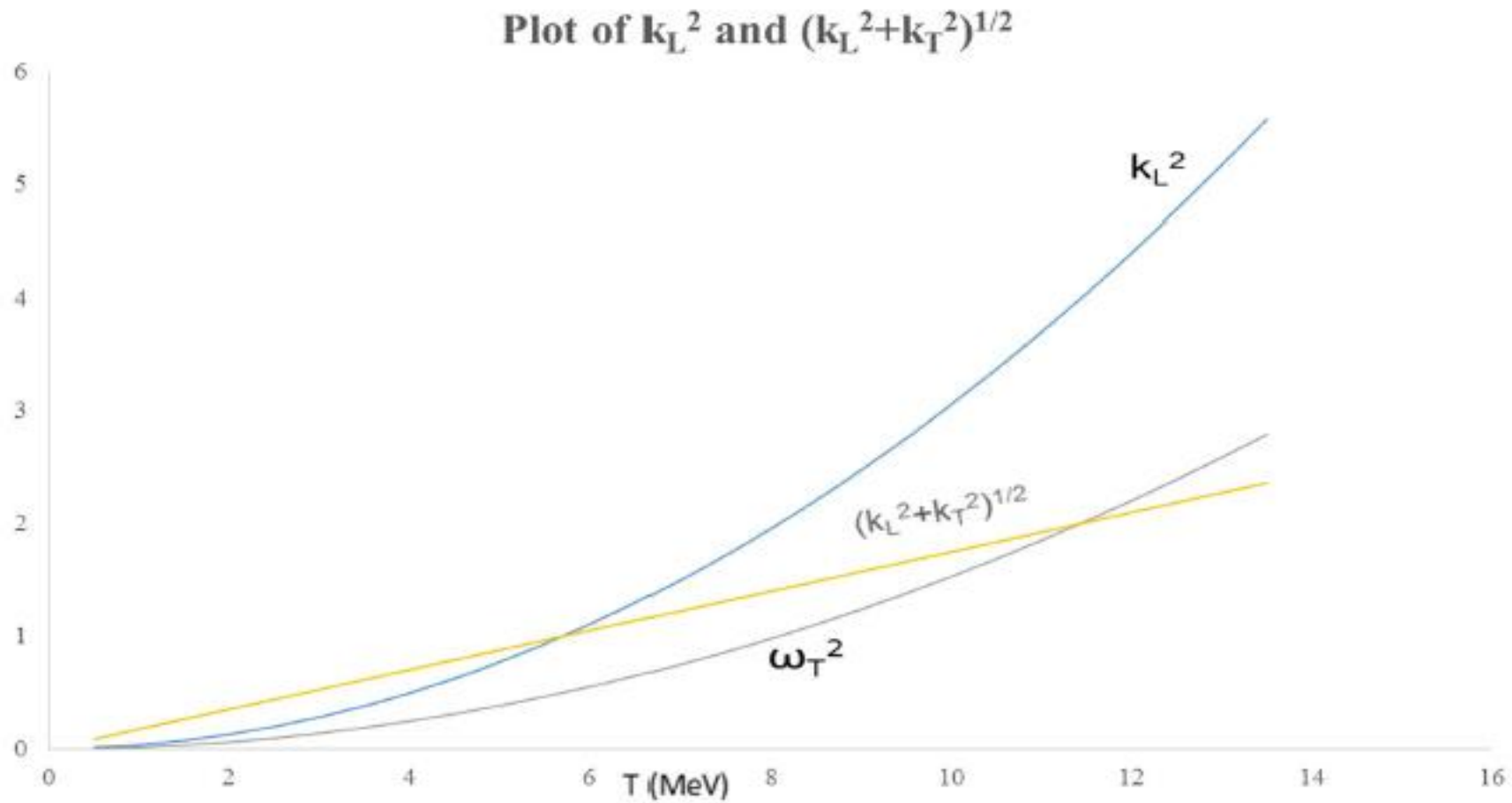


Fig. 3 Comparison of the plots of k ; the magnitude of the propagation vector, longitudinal propagation k_L^2 and transverse frequency ω_T^2



Temperature dependence of QED parameters

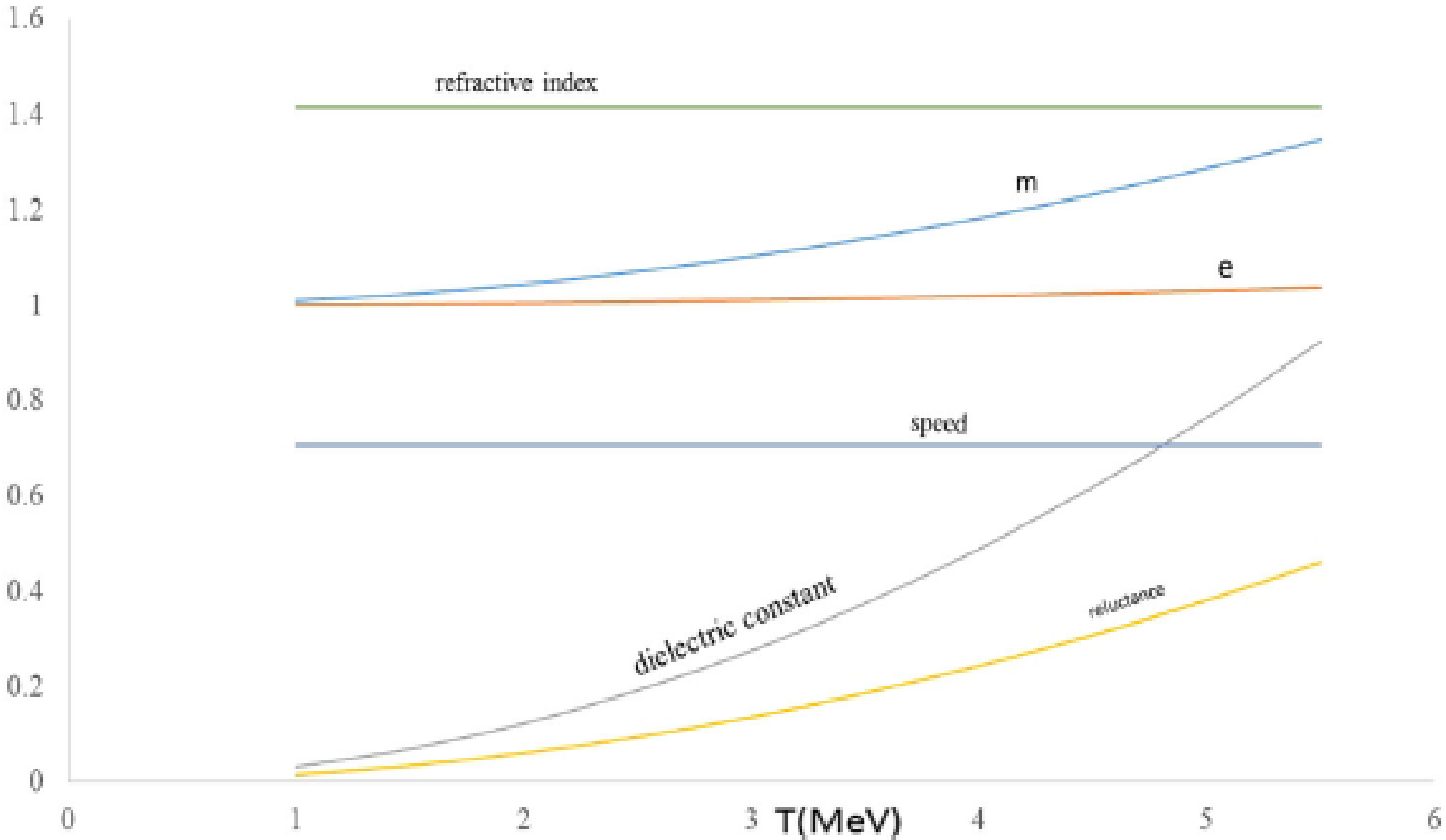


Fig. 5 All of the plasma parameters are plotted as functions of temperature such that the reluctance, propagation speed, and dielectric constant all increase with temperature



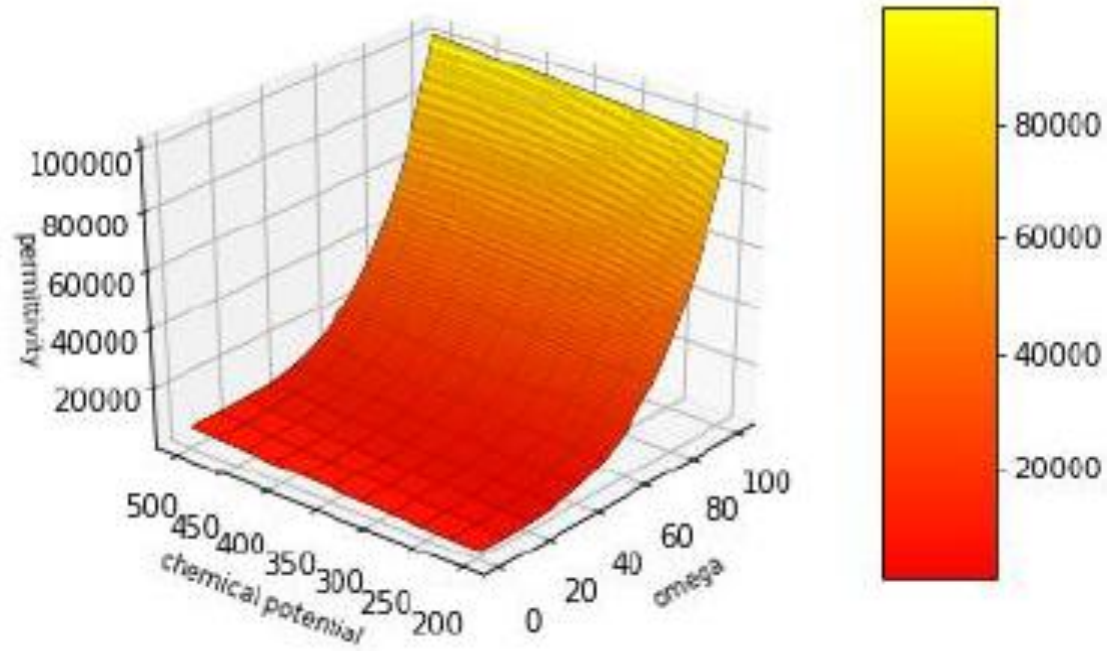


Figure 1: Relative permittivity ϵ_R is plotted versus omega ω in units of electron mass m_e for constant k



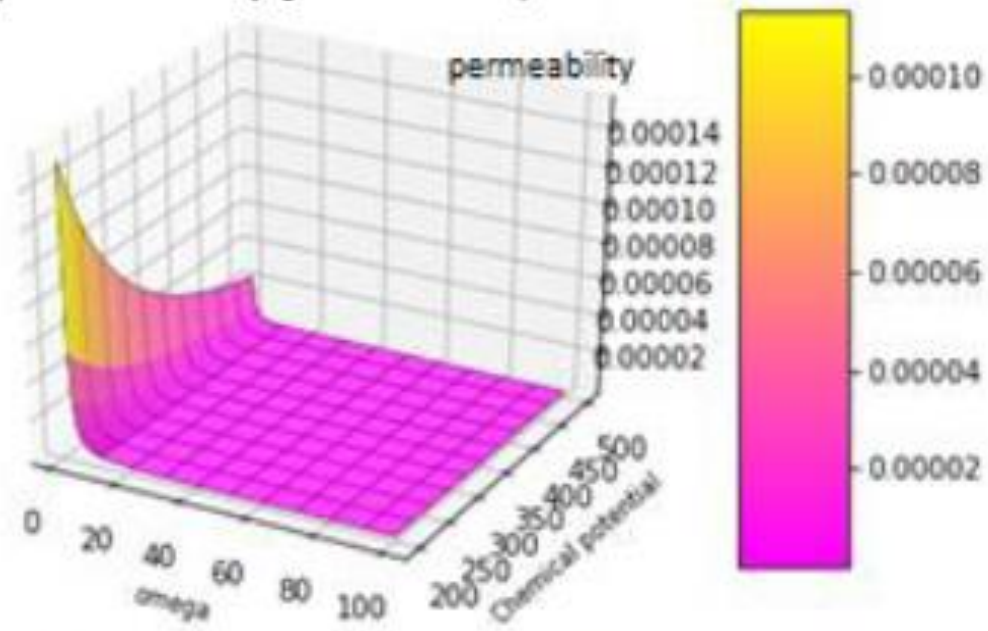


Figure 2: Relative permeability μ_B is plotted versus omega ω in units of electron mass m_e for constant k



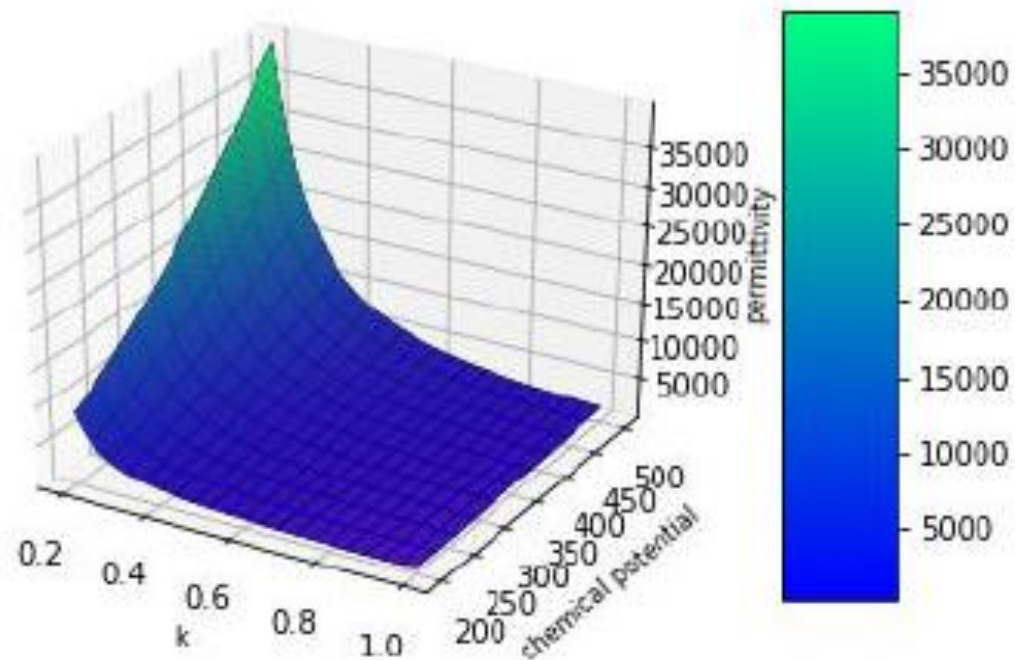


Figure 3: Relative permittivity ϵ_R is plotted versus k in units of electron mass m_e for constant ω



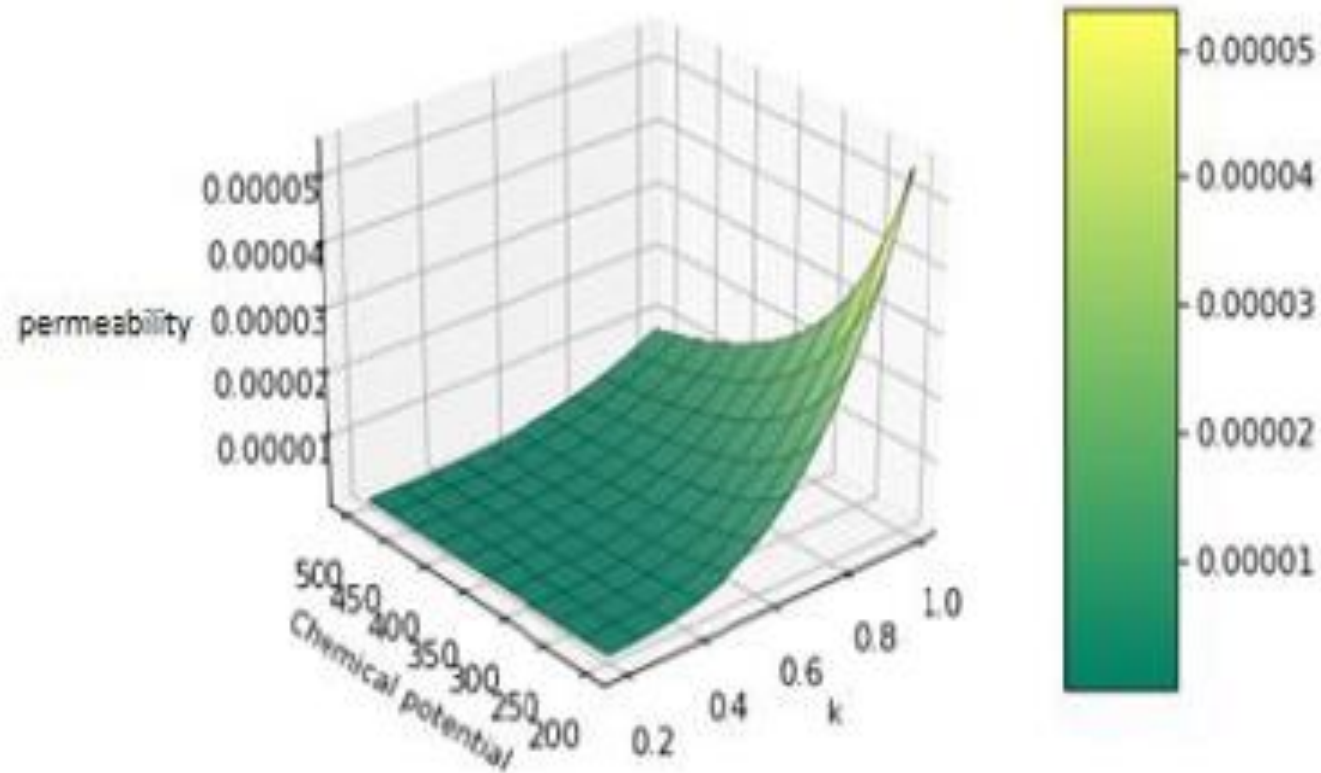


Figure 4: Relative permeability μ_B is plotted versus k in units of electron mass m_e for constant ω



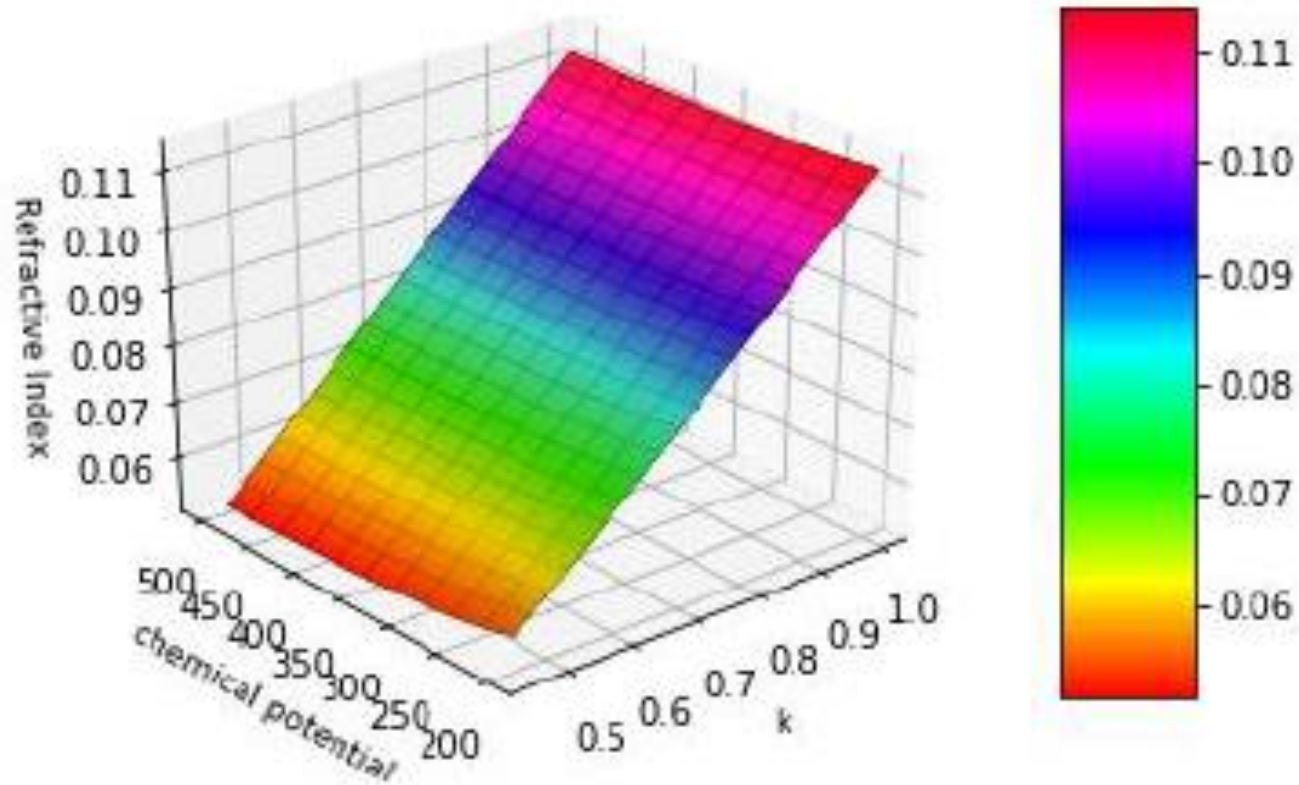


Figure 6: Index of refraction is plotted versus k in units of electron mass m_e for constant ω



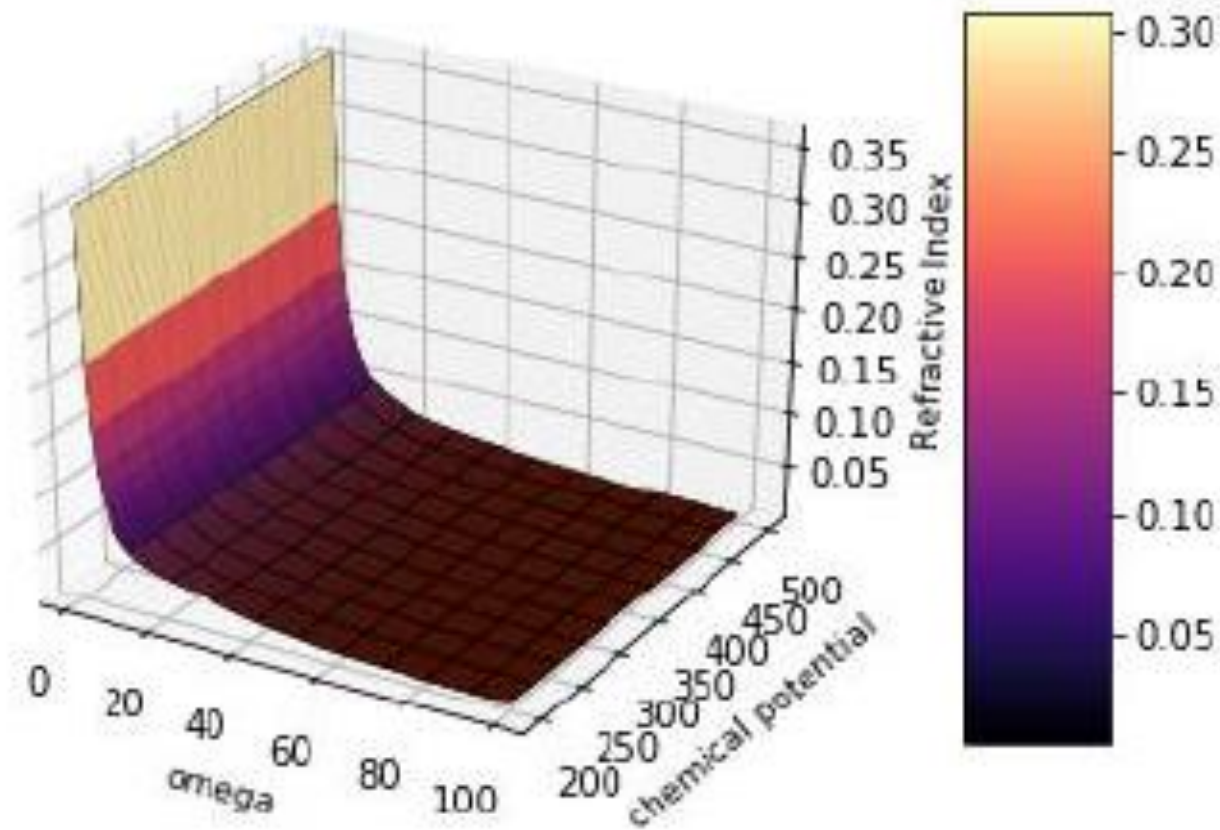
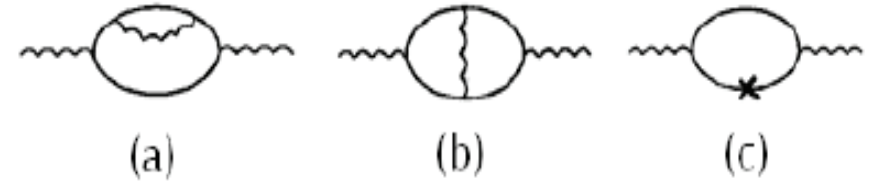


Figure 5: Index of refraction is plotted versus ω in units of electron mass m_e for constant k



Second order Vacuum Polarization



$${}^2\Pi_{\mu\nu}^a(p) = e^4 \int \frac{d^4k}{(2\pi)^4} \int \frac{d^4q}{(2\pi)^4} \\ \times \text{Tr} [\gamma_\mu S_\beta(k) \gamma_\rho D_\beta^{\rho\sigma}(q-k) S_\beta(q) \gamma_\sigma S_\beta(k) \gamma_\nu S_\beta(p-k)] ,$$

$${}^2\Pi_{\mu\nu}^b(p) = e^4 \int \frac{d^4k}{(2\pi)^4} \int \frac{d^4q}{(2\pi)^4} \\ \times \text{Tr} [\gamma_\mu S_\beta(k) \gamma_\rho D_\beta^{\rho\sigma}(q-k) S_\beta(q) \gamma_\nu S_\beta(q-p) \gamma_\sigma S_\beta(k-p)] .$$

$$P_{\mu\nu} = (g_{\mu\nu} - u_\mu u_\nu) + \frac{1}{|\mathbf{p}|^2} (p_\mu - \omega u_\mu)(p_\nu - \omega u_\nu) \quad Q_{\mu\nu} = \frac{1}{p^2 |\mathbf{p}|^2} [\{p^2 u_\mu + \omega(p_\mu - \omega u_\mu)\} \{p^2 u_\nu + \omega(p_\nu - \omega u_\nu)\}]$$



Electromagnetic Properties of a Thermal Medium

$$\omega_L^2 \longrightarrow \lim_{|\mathbf{p}| \rightarrow 0} \Pi_L(|\mathbf{p}|, |\mathbf{p}|, T) = 0,$$

$$\omega_T^2 \longrightarrow \lim_{|\mathbf{p}| \rightarrow 0} \Pi_T(|\mathbf{p}|, |\mathbf{p}|, T) = \frac{\alpha^2 T^2}{6}.$$



(a)



(b)



(c)

QED coupling constant

$$\alpha_R = \alpha(T=0) \left(1 + \frac{\alpha^2 T^2}{6m^2}\right).$$

Electric Permittivity

$$\begin{aligned} \varepsilon(p, T) &= 1 - |\mathbf{p}|^2 \Pi_L(p, T) \\ &= 1 - \frac{2\alpha^2 T^2 p^2}{3} \left(1 + \frac{p_0^2}{2m^2}\right), \end{aligned}$$

Magnetic Permeability

$$\begin{aligned} \frac{1}{\mu(p, T)} &= 1 + \frac{1}{p^2} \left[\Pi_T(p, T) - \frac{p_0^2}{|\mathbf{p}|^2} \Pi_L(p, T) \right] \\ &= 1 + \frac{\alpha^2 T^2}{3} \left[\frac{1}{2p^2} - \frac{1}{|\mathbf{p}|^2} \left(1 + \frac{p_0^2}{2m^2}\right) \left(1 + \frac{2p_0^2}{|\mathbf{p}|^2}\right) \right]. \end{aligned}$$

SM and Mahnaz Haseeb, Int. J. Mod. Phys. A23:4709-4719, 2008.

Mahnaz Haseeb and SM, Phys. Lett. B704:66, 2011.



| T/m | $\delta m/m$ | $\Delta e/e$ | Electron dipole moment | Neutrino dipole moment | Ratio of magnetic moments |
|-------|--------------|--------------|------------------------|------------------------|---------------------------|
| 1.1 | 0.013879 | 2.34E-07 | 0.009252 | 4.03333E-10 | 4.36E-08 |
| 1.5 | 0.025808 | 8.1E-07 | 0.017205 | 7.5E-10 | 4.36E-08 |
| 2 | 0.04588 | 2.56E-06 | 0.030587 | 1.33333E-09 | 4.36E-08 |
| 2.5 | 0.071688 | 6.25E-06 | 0.047792 | 2.08333E-09 | 4.36E-08 |
| 3 | 0.10323 | 1.3E-05 | 0.06882 | 0.000000003 | 4.36E-08 |

Masood, S.S. Eur. Phys. J. C (2017) 77: 826. <https://doi.org/10.1140/epjc/s10052-017-5398-0>



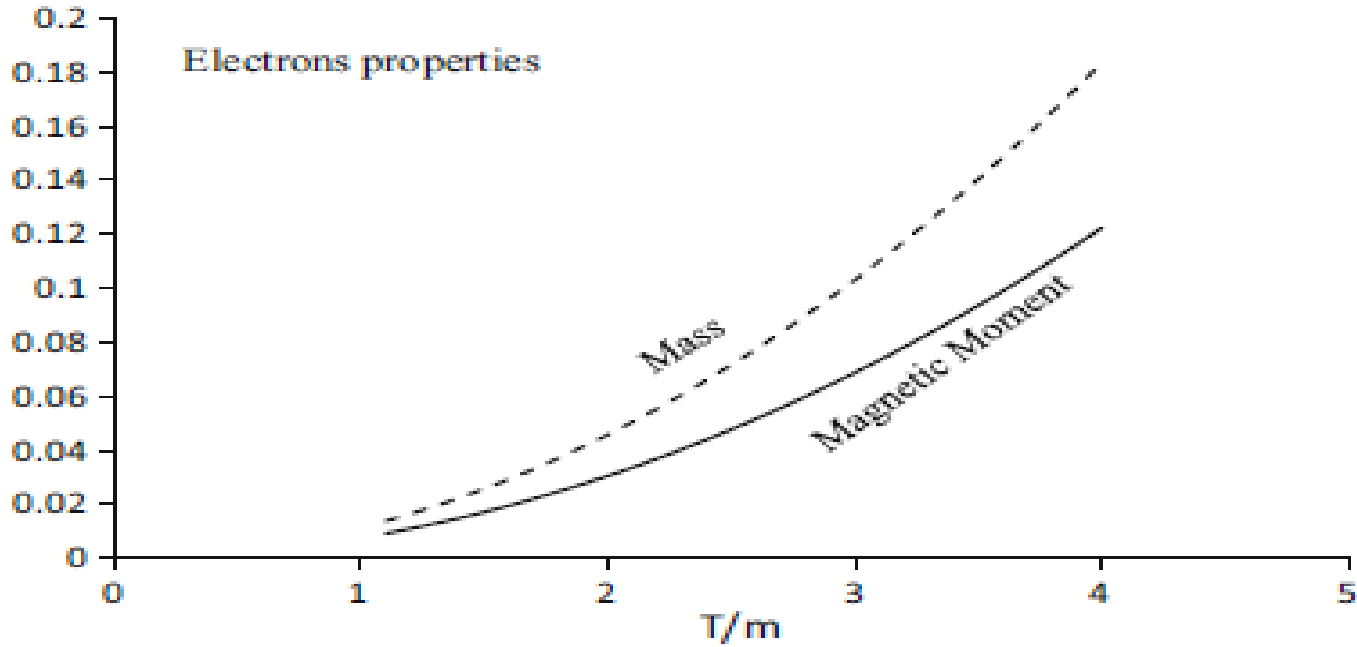


Fig. 3 A comparison of temperature dependent self-mass and the corresponding magnetic moment of the electron shows that the behavior of magnetic dipole moment at finite temperature is exactly similar to the mass of the electron at high temperatures, i.e; $T > m$



Electromagnetic Properties of Hot and Dense Media

For Temperatures smaller than the Chemical Potential



$$\epsilon(K, \mu) = 1 - \frac{2\alpha}{\pi K^3} \left[\mu^2 \omega \left[1 - \frac{m^2}{\mu^2} \right] \ln \frac{\omega - k}{\omega + K} - A_1 \ln \frac{\mu}{m} + \frac{1}{2m^2} \left[\frac{m^2}{\mu^2} - 1 \right] A_2 \right]$$

$$\frac{1}{\mu(K)} = 1 + \frac{2\alpha}{\pi k K^2} \left\{ \frac{1}{4} \left[1 - \frac{m^2}{\mu^2} \right] \left[\frac{k\mu^2}{2} + \frac{k^3}{12} \left[1 - \frac{3\omega^2 + k^2}{4m^2} \right] + \frac{5m^2\omega^2 k}{2k^2} + \frac{3m^2 k}{8} - \omega\mu^2 \left[1 - \frac{m^2}{\mu^2} \right] \left[1 - \frac{\omega^2}{k^2} \right] \left[\frac{\omega^2}{k^2} + \frac{1}{4} \right] \ln \frac{\omega - k}{\omega + k} - \frac{\omega^2}{k^2} \left[1 - \frac{\omega^2}{k^2} \right] - \frac{1}{2} \left[\frac{\omega^2}{k^2} + 1 \right] A_1 \ln \frac{\mu}{m} + \frac{A_2}{4m^2} \left[1 - \frac{m^2}{\mu^2} \right] \left[1 + \frac{2\omega^2}{k^2} \right] \left[1 - \frac{\omega^2}{k^2} \right] \right\}.$$

$$T \ll 4\pi\sigma \ll \frac{1}{a}$$

$$\alpha \equiv 2a(4\pi\sigma)$$

Samina Masood, Phys. Rev. D44, 3943 (1991).

Samina Masood, Phys. Rev. D47, 648 (1993)



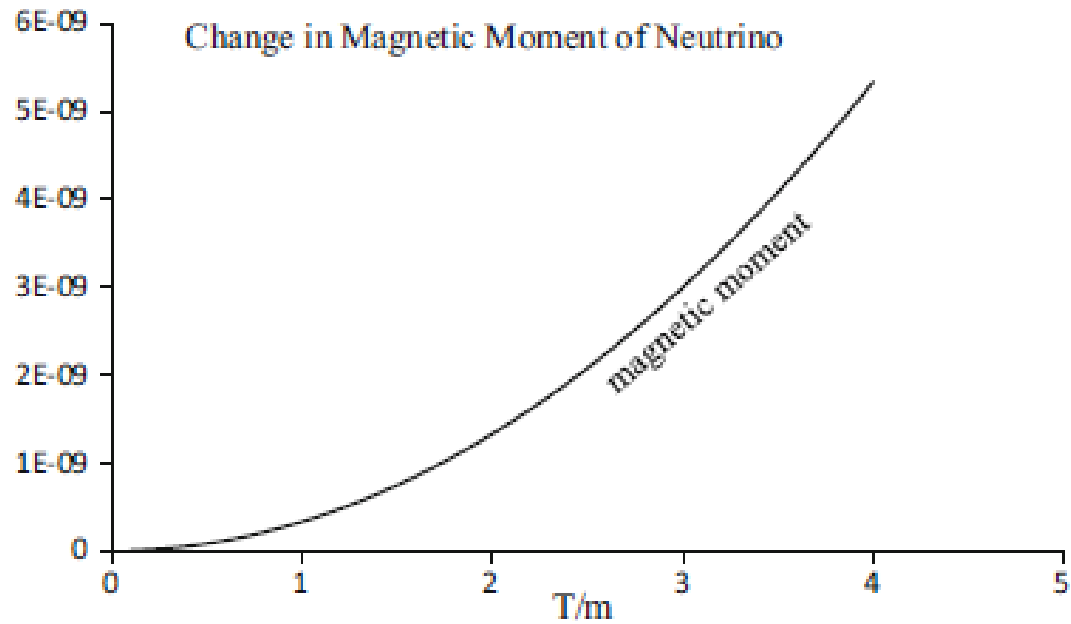


Fig. 4 The ratio of (thermal) electrons background corrections to the magnetic moment of the electronic type neutrino with the corresponding vacuum value of the magnetic moment is plotted as a function of temperature below the neutrino decoupling temperature to extract the pure background effect



Lecture 3: Effect of Electron mass on different parameters

- Magnetic moment of electron
- Electromagnetic properties of particles that propagate in the presence of electron
- Effect on weak interaction processes (involving electrons) such as beta decay
- Decay rates and crosssections of particles



Number density of charged particles

$$N_{\pm} = \frac{1}{2\pi^2} \int_m^{\infty} E^2 dE n_F^{\pm}(E) - \frac{m^2}{4\pi^2} \int_m^{\infty} dE n_F^{\pm}(E) - \frac{m^4}{16\pi^2} \int_m^{\infty} \frac{dE}{E^2} n_F^{\pm}(E) .$$

Average energy density of charged particles

$$N_{\pm} \langle E_{\pm} \rangle = \frac{1}{2\pi^2} \left[\int_m^{\infty} E^3 dE n_F^{\pm}(E) - \frac{m^2}{2} \int_m^{\infty} E dE n_F^{\pm}(E) - \frac{m^4}{4} \int_m^{\infty} \frac{dE}{E} n_F^{\pm}(E) \right] .$$



Number Density of electron

$$a(m\beta, \pm\mu) = \ln(1 + e^{-(m\pm\mu)\beta}),$$

$$b(m\beta, \pm\mu) = \sum_{n=1}^{\infty} (-1)^n e^{\mp n\beta\mu} \text{Ei}(-nm\beta),$$

$$c(m\beta, \pm\mu) = \sum_{n=1}^{\infty} \frac{(-1)^n}{n^2} e^{-n(m\pm\mu)\beta},$$

$$d(m\beta, \pm\mu) = \sum_{n=1}^{\infty} \frac{(-1)^n}{n^3} e^{-n(m\pm\mu)\beta},$$

$$f(m\beta, \pm\mu) = \sum_{n=1}^{\infty} \frac{(-1)^n}{n^4} e^{-n(m\pm\mu)\beta},$$

$$g(m\beta, \pm\mu) = \sum_{n=1}^{\infty} (-1)^n \left[\beta n \text{Ei}(-nm\beta) + \frac{e^{-nm\beta}}{m} \right] e^{\mp n\beta\mu},$$

$$h(m\beta, \pm\mu) = - \sum_{n=1}^{\infty} (-1)^n \left[\frac{\beta^2 n^2}{2} \text{Ei}(-nm\beta) + n\beta \frac{e^{-nm\beta}}{m} \right] e^{\mp n\beta\mu}$$

$$N_{\pm} = \frac{1}{2\pi^2} \left[\frac{m^2}{2\beta} a(m\beta, \mp\mu) + \frac{m}{\beta^2} c(m\beta, \mp\mu) + \frac{1}{\beta^3} d(m\beta, \mp\mu) - \beta \frac{m^4}{8} g(m\beta, \mp\mu) - \frac{m^3}{8} e^{-nm\beta} e^{\pm n\beta\mu} \right],$$

Average Energy Density

$$N_{\pm} \langle E_{\pm} \rangle = \frac{1}{2\pi^2} \left[\frac{m^3}{2\beta} a(m\beta, \mp\mu) - \frac{m^4}{8} b(m\beta, \mp\mu) + \frac{m^2}{2\beta^2} c(m\beta, \mp\mu) + \frac{m}{\beta^3} d(m\beta, \mp\mu) + \frac{1}{\beta^4} f(m\beta, \mp\mu) \right].$$



In a dense symmetric background, these functions attain the form

$$\tilde{a}(m_\ell\beta, \mu) \simeq \frac{1}{2} \ell n [(1 + e^{-\beta(m_\ell - \mu)}) (1 + e^{-\beta(m_\ell + \mu)})]$$

$$\tilde{b}(m_\ell\beta, \mu) \simeq \sum_{n=1}^{\infty} (-1)^n \cosh(n\beta\mu) \text{Ei}(-nm_\ell\beta)$$

$$\tilde{c}(m_\ell\beta, \mu) \simeq \sum_{n=1}^{\infty} (-1)^n \cosh(n\beta\mu) \frac{e^{-n\beta m_\ell}}{n^2}$$

$$\tilde{h}(m_\ell\beta, \mu) \simeq \sum_{n=1}^{\infty} (-1)^{1+n} \left(\frac{\beta^2 n^2}{2} \text{Ei}(-nm_\ell\beta) + n\beta \frac{e^{-n\beta m_\ell}}{m_\ell} \right) \cosh(n\beta\mu)$$



$$a(m\beta, -\mu) \xrightarrow{\mu > T} a'(m\beta, \mu) = \mu - m - \sum_{l=0}^{\infty} \frac{(-1)^n}{(n\beta)^{1-l}} e^{-n\beta(m-\mu)},$$

$$b(m\beta, -\mu) \xrightarrow{\mu > T} b'(m\beta, -\mu) = \ln \mu / m,$$

$$c(m\beta, -\mu) \xrightarrow{\mu > T} c'(m\beta, -\mu) = \frac{\mu^2 - m^2}{2} - \sum_{l=0}^{\infty} \frac{(-1)^l}{\mu^l} l \sum_{n=1}^{\infty} \frac{(-1)^n}{(n\beta)^l} e^{-en\beta(m-\mu)},$$

$$d(m\beta, -\mu) \xrightarrow{\mu > T} d'(m\beta, -\mu) = \frac{\mu^3 - m^3}{3} - \sum_{l=0}^{\infty} \frac{(-1)^l}{\mu^l} \sum_{n=1}^{\infty} \frac{(-1)^n}{(n\beta)^l} e^{-n\beta(m-\mu)},$$

$$f(m\beta, -\mu) \xrightarrow{\mu > T} f'(m\beta, -\mu) = \frac{\mu^4 - m^4}{3} - \sum_{l=0}^{\infty} \frac{(-1)^l}{\mu^l} \sum_{n=1}^{\infty} \frac{(-1)^n}{(n\beta)^{l+2}} e^{-n\beta(m-\mu)},$$

$$g(m\beta, -\mu) \xrightarrow{\mu > T} g'(m\beta, -\mu) = \frac{\mu^{-3} - m^{-3}}{3} - \sum_{l=0}^{\infty} (-1)^l / \mu^l \sum_{n=1}^{\infty} \frac{(-1)^n}{(n\beta)^{l+3}} e^{-n\beta(m-\mu)},$$

$$h(m\beta, -\mu) \xrightarrow{\mu > T} h'(m\beta, -\mu) = \frac{\mu^{-4} - m^{-4}}{4} - \sum_{l=0}^{\infty} \frac{(-1)^l}{\mu^l} \sum_{n=1}^{\infty} \frac{(-1)^n}{(n\beta)^l} + 4e^{-n\beta(m-\mu)}.$$



Corresponding functions for superdense systems; temperature is ignorable as compared to density

$$a'(m\beta, \mu) = \mu - m, \quad b'(m\beta, \mu) = \ln \frac{\mu}{m}, \quad c'(m\beta, \mu) = \frac{\mu^2 - m^2}{2}$$

$$d'(m\beta, -\mu) = \frac{\mu^3 - m^3}{3}, \quad f'(m\beta, -\mu) = \frac{\mu^4 - m^4}{4},$$

$$g'(m\beta, \mu) = \frac{\mu^{-3} - m^{-3}}{3}, \quad h'(m\beta, \mu) = \frac{\mu^{-4} - m^{-4}}{4}.$$



number density

$$N_+ = 0 ,$$

$$N_- = \frac{1}{2\pi^2} \left[\frac{\mu^3 - m^3}{3} - \frac{m^2}{2}(\mu - m) - \frac{m^4}{8} \left[\frac{1}{\mu} - \frac{1}{m} \right] \right] ,$$

average energy density

$$N_+ \langle E_+ \rangle = 0 ,$$

$$N_- \langle E_- \rangle = \frac{1}{2\pi^2} \left[\frac{\mu^4 - m^4}{4} - \frac{m^2}{2} \left[\frac{\mu^2 - m^2}{2} \right] - \frac{m^4}{4} \ln \frac{\mu}{m} \right] ,$$



Neutrinos in a Medium

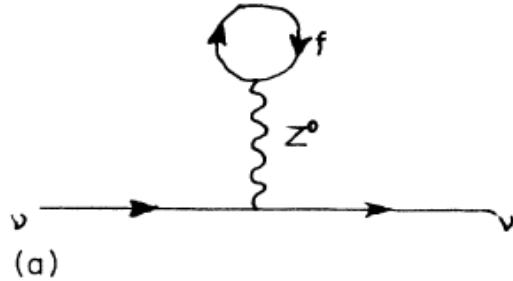
- Weyl neutrino being a massless neutral particle does not respond to any interaction other than weak
- It shows a magnetic moment that is basically induced by the charged particle coupling.
- Massive neutrino could get Dirac or Majorana masses
- Massive neutrinos exhibit more electromagnetic properties and interact with the background differently changing its structure functions.
- Mainly Dirac neutrino is considered
- Number density, Average energy density,



Propagation of Dirac neutrino in a medium

$$\Sigma(k) = m_\nu - (a_L \not{k} + b_L \not{\mathcal{A}} + c_L [\not{k}, \not{\mathcal{A}}]) \frac{1}{2} (1 - \gamma_5)$$

Satisfy Dirac Equation

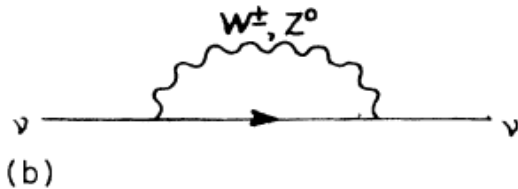


$$c_L = 0 \text{ (NR)}$$

$$|k| = nw$$

$$k^2 = w^2 - |k|^2 \simeq m^2 - 2b_L w$$

$$n = 1 - \frac{m^2}{2w^2} + \frac{b_L}{w} \quad n \text{ is the refractive index}$$



$$\Delta E_{\text{ref}} = \omega_L - \omega_R \approx -b_L$$

$$b_L / w \rightarrow 0$$

FIG. 1. First-order FTD contribution to the self-mass of the neutrino: (a) tadpole graph and (b) bubble graph.



$$\mathcal{M}_\mu = F_D(q^2) \bar{u}_{\nu_1}(p') \gamma_\mu (1 - \gamma_5) u_{\nu_1}(p). \quad f_1(q^2) = F_D(q^2) \quad f_1(0) = F_D(0) = 0.$$

$$f_3(q^2) = F_A(q^2) = \frac{1}{q^2} F_D(q^2)$$

$$\mathcal{M}_\mu = \bar{u}_{\nu_1}(p') \{ \gamma_\mu f_1(q^2) - \gamma_\lambda \gamma_5 [g^\lambda{}_\mu q^2 - q^\lambda q_\mu] f_3(q^2) \} u_{\nu_1}(p)$$

$$\langle r_{\nu_1}^2 \rangle = -6 \left. \frac{\partial f_1(q^2)}{\partial q^2} \right|_{q^2=0} = -6 \left. \frac{\partial F_D(q^2)}{\partial q^2} \right|_{q^2=0}$$

$$a_{\nu_1} = f_3(0) = \left. \frac{F_D(q^2)}{q^2} \right|_{q^2=0} = \left. \frac{\partial F_D(q^2)}{\partial q^2} \right|_{q^2=0}.$$

$$a_{\nu_1} = \frac{1}{6} \langle r_{\nu_1}^2 \rangle.$$



$$\bar{a}_i(m\beta, \mu) = \frac{1}{2}[a_i(m\beta, -\mu) + a_i(m\beta, +\mu)]$$

Similarly, if the neutrons are there in the medium, they will contribute to the refractive energy as

$$(\Delta E_{\text{ref}})_n \simeq \mp \frac{G_F}{\sqrt{2}\pi^2} \left[\frac{m^3}{2\beta} \bar{a}(m\beta, \mu) + \frac{m^2}{2\beta^2} \bar{c}(m\beta, \mu) + \frac{m}{\beta^3} \bar{d}(m\beta, \mu) + \frac{1}{\beta^4} \bar{f}(m\beta, \mu) - \frac{m^4}{8} \bar{b}(m\beta, \mu) \right]$$

$$m_p = m_n \quad (\Delta E_{\text{ref}})_p = \pm (1 - 4 \sin^2 \theta_W) (\Delta E_{\text{ref}})_n \quad \text{Very small for } \sin^2 \theta_W \approx 0.23$$

$$(\Delta E_{\text{ref}})_e \simeq \pm \frac{\sqrt{2}G_F}{\pi^2} \left\{ (1 + 2 \sin^2 \theta_W) \left[\frac{m^3}{2\beta} \bar{a}(m\beta, \mu) + \frac{m^2}{2\beta^2} \bar{c}(m\beta, \mu) + \frac{m}{\beta^3} \bar{d}(m\beta, \mu) + \frac{1}{\beta^4} \bar{f}(m\beta, \mu) - \frac{m^4}{8} \bar{b}(m\beta, \mu) \right] - \frac{8w}{3m_W^2} \left[\frac{m^3}{2\beta} \bar{a}(m\beta, \mu) - \frac{m^4}{8} \bar{b}(m\beta, \mu) + \frac{m^2}{2\beta^2} \bar{c}(m\beta, \mu) + \frac{m}{\beta^3} \bar{d}(m\beta, \mu) + \frac{1}{\beta^4} \bar{f}(m\beta, \mu) \right] \right\}$$

In the presence of the charged leptons of the same flavor in the heat bath (ignoring their polarization), the refractive energy of the corresponding ν turns out to be



Refractive energy in terms of

mass, temperature and the chemical potential of the background

Refractive energy of neutrinos in the presence of all flavors hot neutrino background

$$(\Delta E_{\text{ref}})_{\nu_l} \simeq \pm \frac{\sqrt{2}G_F}{\pi^2} \left[\frac{m^3}{2\beta} \bar{a}(m\beta, \mu) + \frac{m^2}{2\beta^2} \bar{c}(m\beta, \mu) + \frac{m}{\beta^3} \bar{d}(m\beta, \mu) \right]$$
$$\bar{a}_i(m\beta, \mu) = \frac{1}{2}[a_i(m\beta, -\mu) - a_i(m\beta, +\mu)]$$

Refractive energy of neutrinos in the presence of hot neutrino background of the same flavor

$$(\Delta E_{\text{ref}})_{\nu_l} \simeq \pm \frac{\sqrt{2}G_F}{\pi^2} \left[\frac{m^2}{2\beta} \bar{a}(m\beta, \mu) + \frac{m}{\beta^2} \bar{c}(m\beta, \mu) + \frac{1}{\beta^3} \bar{d}(m\beta, \mu) - \beta \frac{m^4}{8} \bar{g}(m\beta, \mu) - \frac{m^3}{4} e^{-nm\beta} \sinh n\beta\mu \right]$$
$$+ \frac{8\sqrt{2}G_F W}{3m_Z^2 \pi^2} \left[\frac{m^3}{2\beta} \bar{a}(m\beta, \mu) - \frac{m^4}{8} \bar{b}(m\beta, \mu) + \frac{m^2}{2\beta^2} \bar{c}(m\beta, \mu) + \frac{m}{\beta^3} \bar{d}(m\beta, \mu) + \frac{1}{\beta^4} \bar{f}(m\beta, \mu) \right]$$

.Samina S.Masood, Phys.Rev.D48, 3250(1993)



Magnetic Moment and Standard model

- Magnetic moment is intrinsic property of charge only. Neutral point particle particles can get induced magnetic moment
- Magnetic is a property of charge and mass and no form factors.
- Even the standard $SU(2) \times U(1)$ can acquire nonzero magnetic moment only if it has nonzero mass only
- Mass of neutrino needs extension in the standard electroweak model with Weyl neutrino and individual lepton conservation
- We include right handed neutrino in the electroweak model as a singlet just like right handed electron. We call it as Minimal Electroweak Model
- Other model with different mass of neutrino will alter these results.
- In different models couplings and additional diagrams will contribute, depending on the model of extension
- Majorana mass can only acquire the transition magnetic moment



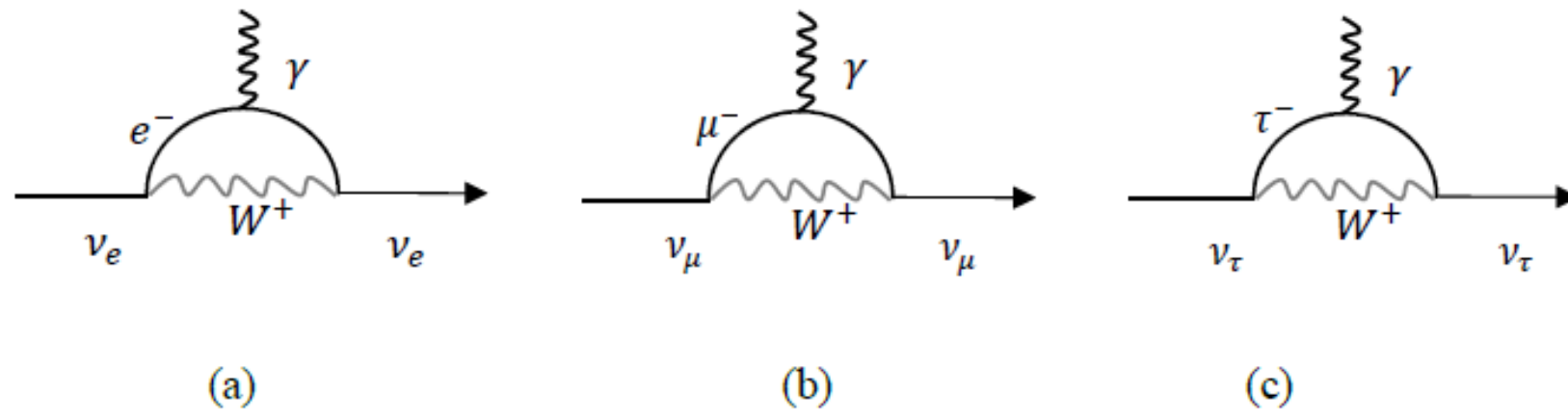


Fig.1: Bubble diagrams for different flavors of neutrinos in the minimal standard model. (a) corresponds to electron-neutrino (b) muon-neutrino and (c) tau-neutrino

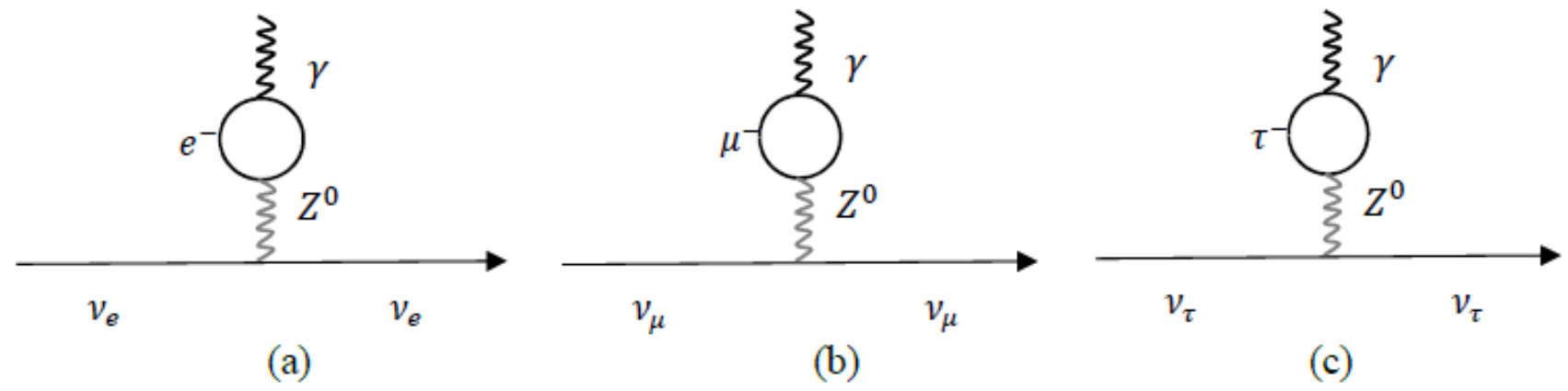


Fig.2: Tadpole diagrams for different flavors of neutrinos in the minimal standard model. (a) corresponds to electron-neutrino (b) muon-neutrino and (c) tau-neutrino



$$-i\Gamma_{\mu}^{(W)} = \frac{1}{2} eg^2 \int \frac{d^4 p}{(2\pi)^4} \gamma^{\alpha} L iS_F(p-q) \gamma_{\mu} iS_F(p) \gamma_{\alpha} L \frac{1}{(p-p')^2 - m_W^2}$$

$$-i\Gamma_{\mu}^{(Z)} = \frac{eg_Z^2}{a^2 - m_Z^2} \gamma^{\alpha} L \int \frac{d^4 p}{(2\pi)^4} \text{Tr}[iS_F(p-q) \gamma_{\mu} iS_F(p) \gamma_{\alpha} (a_Z + b_Z \gamma_5)]$$

$$\gamma^{\alpha} L M \gamma_{\alpha} L = -(\text{Tr} M \gamma_{\alpha} L) \gamma^{\alpha} L \quad \text{and} \quad \frac{g_Z^2}{m_Z^2} \rightarrow \frac{g^2}{2m_W^2}, \quad a_Z \rightarrow \frac{1}{2}, \quad b_Z \rightarrow -\frac{1}{2}$$

Fierz Transformation

$$T_{\mu\nu}^{(Z)} = \frac{eg_Z^2}{m_Z^2} \int \frac{d^4 p}{(2\pi)^3} \text{Tr}[(\not{p} - \not{q} + m) \gamma_{\mu} (\not{p} + m) \gamma_{\nu} (a_Z + b_Z \gamma_5)]$$

$$\Gamma_{\mu}^{(W,Z)} = T_{\mu\nu}^{(W,Z)} \gamma^{\nu} L$$

$$\times \left[\frac{\delta\{(p-q)^2 - m^2\} n_F^+(p-q)}{p^2 - m^2} + \frac{\delta(p^2 - m^2) n_F^+(p)}{(p-q)^2 - m^2} \right]$$



$$\Gamma_\mu = [F_1 \bar{g}_{\mu\nu} \gamma^\nu + F_2 u_\mu + iF_3 (\gamma_\mu u_\nu - \gamma_\nu u_\mu) q^\nu + iF_4 \epsilon_{\mu\nu\alpha\beta} \gamma^\nu q^\alpha u^\beta] L$$

$p_0^2 = p^2 + m^2 + eB(2n + 1)$ L, T and P correspond to the Longitudinal, Transverse and the Polarization components, respectively.

Charge Radius $F_1 = T_T + \frac{\omega}{Q^2}(T_L - T_T)$

Anapole Moment $F_2 = \frac{1}{V^2}(T_L - T_T)$

Electric Dipole Moment $iF_3 = -\frac{\omega}{Q^2}(T_L - T_T)$ $F_3(q^2 = 0) = D_E = -\frac{i\omega}{q^2}(T_L - T_T)$

Magnetic Dipole Moment $F_4 = \frac{T_P}{Q}$ $F_4(q^2 = 0) = D_M = -\frac{T_P}{2q}$



$$T_T = \frac{eg^2}{2M^2} \left(\alpha - \frac{\beta}{u^2} \right)$$

$$T_L = \frac{eg^2 \beta}{M^2 u^2}$$

$$T_P = -\frac{eg^2}{M^2} |q| \kappa$$

$$T_{\mu\nu} = T_T R_{\mu\nu} + T_L Q_{\mu\nu} + T_P P_{\mu\nu}$$

$$\omega = q \cdot u \quad q = (\omega^2 - |q|^2)^{1/2}$$

$$\tilde{a}_i(m_\ell \beta, \mu) = \frac{1}{2} [a_i(m_\ell \beta, \mu) + a_i(m_\ell \beta, -\mu)]$$

$$\bar{a}_i(m_\ell \beta, \mu) = \frac{1}{2} [a_i(m_\ell \beta, \mu) - a_i(m_\ell \beta, -\mu)]$$

$$R_{\mu\nu} \equiv \bar{g}_{\mu\nu} - Q_{\mu\nu}$$

$$Q_{\mu\nu} \equiv \frac{\bar{u}_\mu \bar{u}_\nu}{\bar{u}}$$

$$P_{\mu\nu} \equiv \frac{1}{|q|} \epsilon_{\mu\nu\alpha\beta} q^\alpha u^\beta$$

$$\bar{g}_{\mu\nu} = g_{\mu\nu} - \frac{q_\mu q_\nu}{q^2}$$

$$\bar{u}_\mu = g_{\mu\nu} u^\nu$$

$$u_\mu = (1, 0, 0, 0)$$

$$\bar{a}_i(m_\ell \beta, \mu) \longrightarrow 0$$

For small chemical
potential



$$\begin{aligned}
\alpha &= \int \frac{d^3p}{(2\pi)^3 2E} (n_F^+ + n_F^-) \left[\frac{2m^2 - 2p \cdot q}{q^2 + 2p \cdot q} + (q \leftrightarrow -q) \right] \\
\beta &= \int \frac{d^3p}{(2\pi)^3 2E} (n_F^+ + n_F^-) \left[\frac{2(p \cdot u)^2 - 2(p \cdot u)(q \cdot u) - p \cdot q}{q^2 - 2p \cdot q} + (q \leftrightarrow -q) \right] \\
\kappa &= - \int \frac{d^3p}{(2\pi)^3 2E} (n_F^+ - n_F^-) \left[\frac{1}{q^2 + 2p \cdot q} + (q \leftrightarrow -q) \right] \quad (
\end{aligned}$$

$$\begin{aligned}
\alpha &\simeq \frac{1}{\pi^2} \left[\frac{\tilde{c}(m_\ell \beta, \mu)}{\beta^2} + \frac{m}{\beta} \tilde{a}(m_\ell \beta, \mu) - \frac{m^2}{2} \tilde{b}(m_\ell \beta, \mu) - \frac{m^4 \beta^2}{8} \tilde{h}(m_\ell \beta, \mu) \right] \\
\beta &\simeq \frac{1}{\pi^2} \left[\left(1 + \frac{3}{8} \ln \frac{1-v}{1+v} \right) \frac{\tilde{c}(m_\ell \beta, \mu)}{\beta^2} + \frac{m}{\beta} \tilde{a}(m_\ell \beta, \mu) - \frac{m^2}{2} \tilde{b}(m_\ell \beta, \mu) - \frac{m^4 \beta^2}{8} \tilde{h}(m_\ell \beta, \mu) \right] \\
\kappa &\simeq \frac{1}{\pi^2} \left[\bar{b}(m_\ell \beta, \mu) + m_\ell^2 \bar{h}(m_\ell \beta, \mu) \right]
\end{aligned}$$



$$\alpha \approx \frac{1}{\pi^2} \left[\frac{\tilde{c}(m_\ell \beta, \mu)}{\beta^2} + \frac{m}{\beta} \tilde{a}(m_\ell \beta, \mu) - \frac{m^2}{2} \tilde{b}(m_\ell \beta, \mu) - \frac{m^4 \beta^2}{8} \tilde{h}(m_\ell \beta, \mu) \right]$$

$$\beta \approx \frac{1}{\pi^2} \left[\left(1 + \frac{3}{8} \ln \frac{1-v}{1+v}\right) \frac{\tilde{c}(m_\ell \beta, \mu)}{\beta^2} + \frac{m}{\beta} \tilde{a}(m_\ell \beta, \mu) - \frac{m^2}{2} \tilde{b}(m_\ell \beta, \mu) - \frac{m^4 \beta^2}{8} \tilde{h}(m_\ell \beta, \mu) \right]$$

$$\kappa \approx \frac{1}{\pi^2} \left[\bar{b}(m_\ell \beta, \mu) + m_\ell^2 \bar{h}(m_\ell \beta, \mu) \right]$$

$$\tilde{a}_i(m_\ell \beta, \mu) = \frac{1}{2} [a_i(m_\ell \beta, \mu) + a_i(m_\ell \beta, -\mu)]$$

$$\bar{a}_i(m_\ell \beta, \mu) = \frac{1}{2} [a_i(m_\ell \beta, \mu) - a_i(m_\ell \beta, -\mu)]$$

All of the a, b, c functions vanish in extreme T limit. For $\mu=0$ barred function vanish and for more lepton and less antileptons, tilde functions correspond to corresponding electron



$$a_{\nu_\ell} = \frac{T^2 G_F m_e m_{\nu_\ell}}{12M^2} \mu_B$$

$$a_{\nu_e} = \frac{T^2 G_F m_e m_{\nu_e}}{12M^2} \mu_B \approx 6.58 \times 10^{-16} \mu_B$$

$$a_{\nu_\mu} = \frac{T^2 G_F m_e m_{\nu_\mu}}{12M^2} \mu_B \approx 5.55 \times 10^{-11} \mu_B$$

$$a_{\nu_\tau} = \frac{T^2 G_F m_e m_{\nu_\tau}}{12M^2} \mu_B \approx 4.53 \times 10^{-9} \mu_B$$



Table 1: Magnetic Moment of Charged Leptons around Nucleosynthesis in the Universe

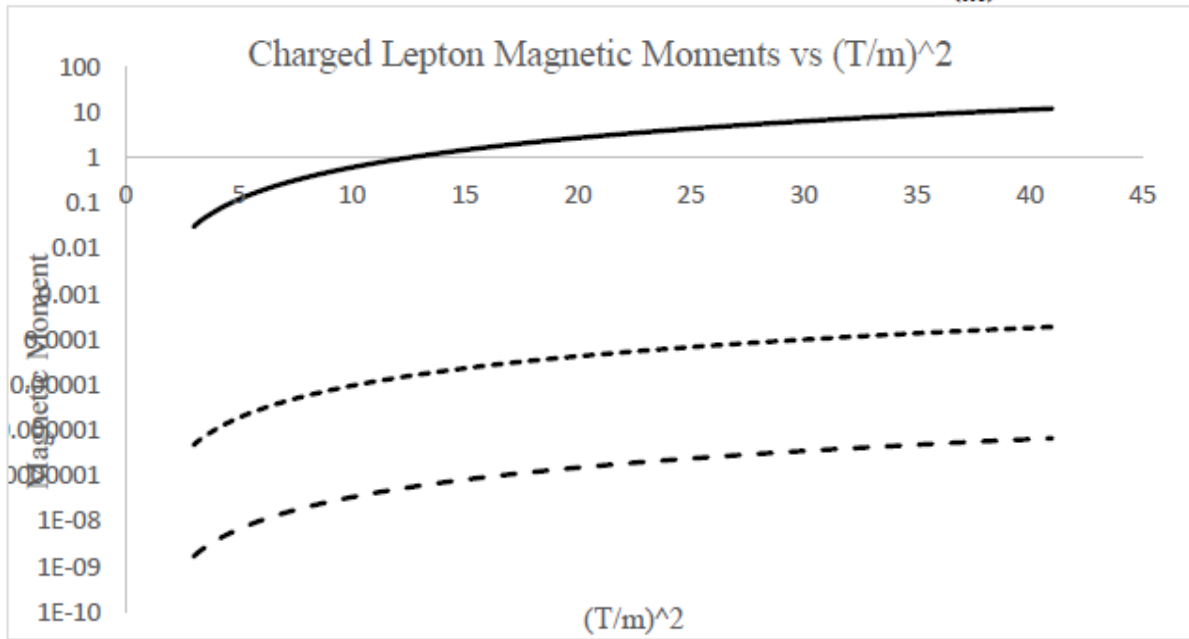
| Charged Leptons | Mass (eV) | Corresponding Temperature (K) | Magnetic Moment at T=0 (μ_B) | Thermal Contribution at T= m_e |
|-----------------|-----------------------|-------------------------------|------------------------------------|----------------------------------|
| e | 0.511×10^6 | 0.592×10^{10} | 1 | $-7.6 \times 10^{-3} \mu_B$ |
| μ | 105.65×10^6 | 0.122×10^{13} | 4.8×10^{-3} | $-1.19 \times 10^{-7} \mu_B$ |
| τ | 1776.82×10^6 | 0.206×10^{14} | 2.8×10^{-4} | $-4.2 \times 10^{-11} \mu_B$ |

Table 2: Magnetic Moment of Neutrinos

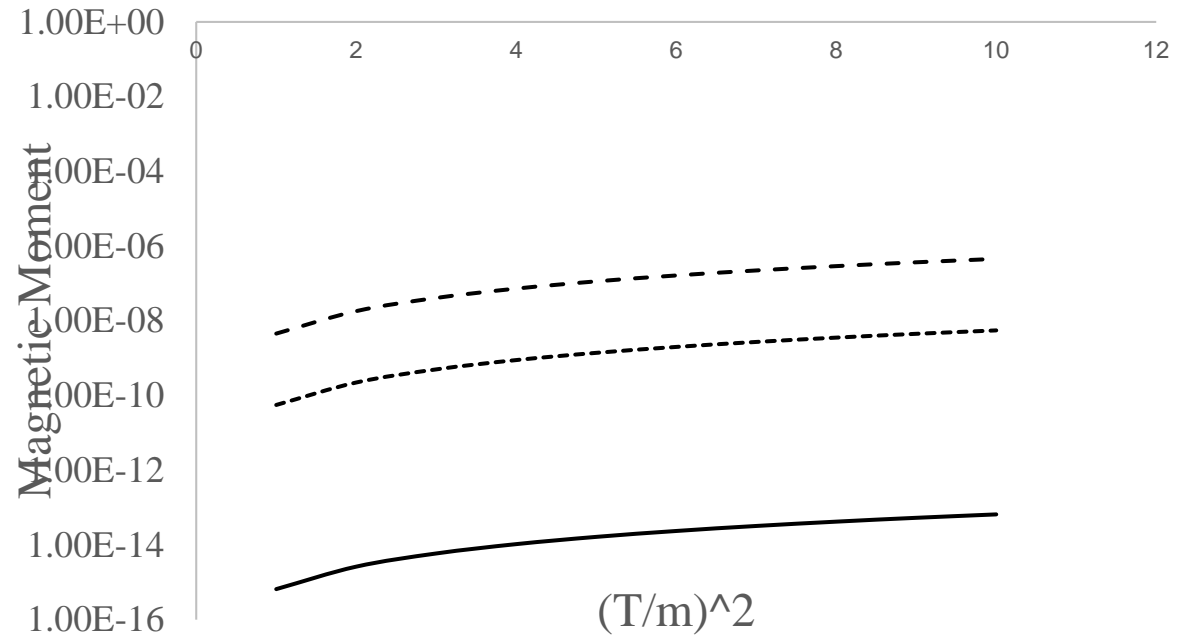
| Neutrino Flavor | Mass (eV) | Corresponding Temperature (K) | Magnetic Moment at T=0 μ_B | Magnetic Moment with Thermal Contribution at T= m_e μ_B |
|-----------------|--------------------|-------------------------------|--------------------------------|---|
| ν_e | 2.25 | 2.6×10^4 | 7.2×10^{-19} | 6.58×10^{-16} |
| ν_μ | 1.9×10^5 | 2.2×10^9 | 6.08×10^{-14} | 5.55×10^{-11} |
| ν_τ | 1.55×10^7 | 2.1×10^{11} | 4.96×10^{-12} | 4.53×10^{-9} |



Figure 4: Charged Lepton Magnetic Moment vs $(\frac{T}{m})^2$



Neutrino Magnetic Moment vs (T/m)²



Polarization diagram contribution

$$\kappa \longrightarrow 0 \text{ as } \mu \longrightarrow 0$$

$$\kappa \simeq -\frac{1}{8\pi^2} \ln \frac{\mu}{m_\ell}$$

$$\alpha_{\nu_\ell}^\beta \simeq \frac{G_F m_\ell}{4\pi^2} m_{\nu_\ell} \left[\tilde{b}(m_\ell \beta, \mu) + \frac{4}{M^2} (m_\ell \tilde{a}(m_\ell \beta, \mu) - \tilde{c}(m_\ell \beta, \mu)) \mu_B \right]$$

$$D_M^{\text{stat}} = \frac{eg^2}{2M^2} \kappa + \alpha_{\nu_\ell}^{\text{stat}}$$

$$D_E^{\text{stat}} = -\frac{i\omega}{q^2} \frac{eg}{2M^2} (3\beta - \alpha)$$

$$a_\nu^{\text{stat}} \simeq \frac{G_F m_\ell}{8\pi^2} m_{\nu_\ell} \ln \frac{\mu}{m_\ell}$$

$$D_M^{\text{stat}} \simeq \left(\frac{G_F m_\ell}{8\pi^2} - \frac{m_\ell g_Z^2}{16M^2} \right) m_{\nu_\ell} \ln \frac{\mu}{m_\ell}$$



$$a_{\nu\ell}^{stat} \simeq \sum_{\ell'}^{\infty} \frac{f_{\ell\ell'} h_{\ell\ell'}}{16\pi^2 m_h^2} m_{\ell'}^2 \tilde{b}(m_{\ell'} \beta, \mu) \mu_B$$

$$f_{e\mu} h_{e\mu} / m_h^2 \simeq 2.8 \times 10^{-6} \text{GeV}^{-2}$$

$$f_{e\tau} h_{e\tau} / m_h^2 \simeq 2.8 \times 10^{-6} \text{GeV}^{-2}$$

$$a_{\nu\ell}^{stat} \simeq \sum_{\ell'=e,\mu,\tau}^{\infty} \frac{f_{\ell\ell'} h_{\ell\ell'}}{16\pi^2 m_h^2} m_{\ell'}^2 \ln \frac{\mu}{m_{\ell'}} \mu_B$$



Effective Magnetic Moment in strong Magnetic Field

$$G^e(x, x') = -\frac{1}{(2\pi^2)\beta} \sum_{n'=0}^{\infty} \sum_{p_4} \int \frac{dp_3 dp_2}{(p_4^{*2} + p_3^2 + m_e^2 + 2eBn')}$$

n' is the Landau number

$$\cdot \{ (ip_4^* \gamma_4 + ip_3 \gamma_3 - m_e) (\sigma_+ \psi_{n'}(\xi) \psi_{n'}(\xi') + \sigma_- \psi_{n'-1}(\xi) \psi_{n'-1}(\xi'))$$

$$+ 1/2 \sqrt{2eBn'} [\gamma_+ \psi_{n'}(\xi) \psi_{n'-1}(\xi') - \gamma_- \psi_{n'-1}(\xi) \psi_{n'}(\xi')] \}$$

$$\cdot \exp[ip_4(x_4 - x'_4) + ip_3(x_3 - x'_3) + ip_2(x_2 - x'_2)],$$

$$\xi = \sqrt{eB}(x_1 + x_o), \xi' = \sqrt{eB}(x'_1 + x_o), x_o = \frac{p_2}{eB}$$

$$\sigma_3 = i/2[\gamma_1, \gamma_2], p_\lambda^* = p_\lambda - i\mu\delta_{4\lambda} \quad \sigma^\pm = 1/2[1 \pm \sigma_3], \gamma_\pm = 1/2[\gamma_1 \pm i\gamma_2]$$



$$D_{\mu\nu}^W(x, x') = \frac{1}{(2\pi)^2\beta} \sum_{p_4} \sum_n \int dp_2 dp_3 \left[\frac{R^- + R^+}{2} \Psi_{\mu\nu}^1 + R^0 \Psi_{\mu\nu}^2 + i \frac{(R^- - R^+)}{2} \Psi_{\mu\nu}^3 \right]$$

$$\Psi_{\mu\nu}^1 = \frac{1}{B^2} G_{\mu\nu}^{02} \cdot \psi_n(\xi) \psi_n(\xi') \exp[ip_4(x_4 - x'_4) + ip_3(x_3 - x'_3) + ip_2(x_2 - x'_2)].$$

$$\Psi_{\mu\nu}^2 = \delta_{\mu\nu} - \frac{1}{B^2} G_{\mu\nu}^{02}$$

$$\Psi_{\mu\nu}^3 = \frac{1}{B} G_{\mu\nu}^0$$

$$E_n^{W2} = M_W^2 + p_3^2 + 2eB(n + 1/2)$$

$$R^\pm = [p_4^{*2} + E_n^{W2} \pm 2eB]^{-1}, \quad R^0 = [p_4^{*2} + E_n^{W2}]^{-1}$$

$G_{\mu\nu}^{02}$ is the field tensor of the $SU(2) \times U(1)$ electromagnetic external field



Contribution of charge current to selfmass of neutrino

P_L is the usual left projection operator.

$$\Sigma^C(x, x') = -i \frac{g^2}{(2\pi)^3} \gamma_\mu G^e(x, x') D_{\mu\nu}^W(x - x') \gamma_\nu$$

$$m_{eff} = \frac{g^2 e |B| \mu_e}{(2\pi)^2 (m_W^2 - e|B|)}$$

Self mass in momentum space from the inverse propagator

$$\Sigma^C(k) = \frac{g^2 e B}{(2\pi)^2} \left(\sum_{p_4} \int dp_3 G_e^o(p_3 + k_3, p_4 + k_4) \Sigma_{\alpha\beta} \right) P_L, \quad d_\nu = \frac{d m_{eff}}{d |B|}$$

Magnetic moment of massless neutrino

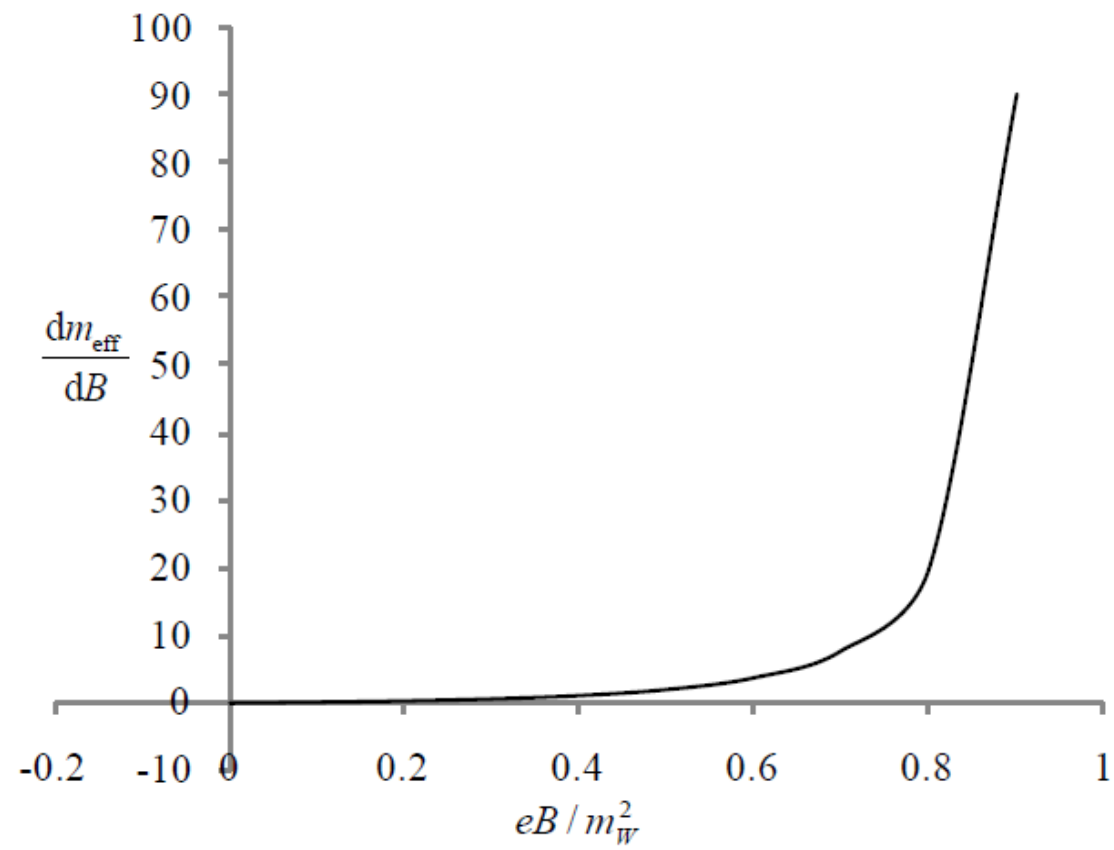
$$d_\nu = g^2 e \mu_e / m_W^2 = 0.79 \times 10^{-10} \mu_B$$

$$d_\nu = 0.79 \times 10^{-10} \mu_B \text{ for } B_m \sim 10^{12} - 10^{14}$$

$$\mu_e = 2\pi^2 N_e / eB.$$

$B \ll m_W$ and extremely large
chemical potential of electron





$$m_{eff} = \frac{g^2 e |B| \mu_e}{(2\pi)^2 (m_W^2 - e |B|)}$$

$$|B| \prec \frac{m_W^2}{e} = 10^{24} \text{ Gauss}$$

$$a_{\nu\ell}^B = \frac{3G_F^2}{4\sqrt{2}\pi^4} \frac{e |B| \mu_e}{(1 - \frac{e|B|}{m_W^2})} \mu_B$$

Using effective mass of Weyl neutrino

$$a_{\nu\ell}^B \simeq 2 \times 10^{-15} \mu_B$$

$$\mu_e \simeq 100 m_e$$

$$eB \simeq 0.9 m_W^2$$

$$\frac{dm_{eff}}{dB} = \frac{g^2 e \mu_e m_W^2}{(2\pi)^2 (m_W^2 - e |B|)^2}$$

$$(a_{\nu\ell}^B)_{eff} \equiv \frac{dm_{eff}}{dB}$$

$$(a_{\nu\ell}^B)_{eff} \longrightarrow 10^{-12}$$

In the limit of $B \rightarrow 0$ Effective Magnetic Moment approaches to the cosmological limit



Quantum Magnetic Collapse

We study the thermodynamics of degenerate electron and charged vector boson gases in very intense magnetic fields. In degenerate conditions of the electron gas, the pressure transverse to the magnetic field B may vanish, leading to a transverse collapse. For W bosons an instability arises because the magnetization diverges at the critical field $B_c = M_W^2/e$. If the magnetic field is self-consistently maintained, the maximum value it can take is of the order of $2B_c/3$, but in any case the system becomes unstable and collapses.



The one-loop thermodynamical potential per unit volume of the electron-positron sector is $\Omega_e = \Omega_{se} + \Omega_{0e}$,

Quantum Magnetic Collapse

$$\Omega_W = \Omega_{sW} + \Omega_{0W}$$

Number Density

$$N_e = \frac{eB}{4\pi^2} \sum_0^\infty a_n \left[\int_{-\infty}^{\infty} dp_3 (n_e^+ - n_e^-) \right], \quad N_W = \frac{eB}{4\pi^2} \left[\int_{-\infty}^{\infty} dp_3 (n_{0p}^+ - n_{0p}^-) \right] + \frac{eB}{4\pi^2} \sum_0^\infty b_n \left[\int_{-\infty}^{\infty} dp_3 (n_p^+ - n_p^-) \right]$$

Magnetization

$$\mathcal{M}_{W,e} = -\partial \bar{\Omega}_{W,e} / \partial B, \quad \mathcal{M}_e = -\frac{\Omega_{se}}{B} - \frac{e}{4\pi^2} \sum_0^\infty a_n \left[\int_{-\infty}^{\infty} dp_3 \frac{eBn}{E_q} (n_e^+ + n_e^-) \right] + \mathcal{M}_{0e},$$

$$\mathcal{M}_{0e,0W} = -\partial \Omega_{0e,0W} / \partial B$$

$$\mathcal{M}_e = \frac{e}{4\pi^2} \sum_0^{n_p} a_n \left(\mu_e \sqrt{\mu_e^2 - m^2 - 2eBn} - (m^2 + 4eBn) \ln \frac{\mu_e + \sqrt{\mu_e^2 - m^2 - 2eBn}}{\sqrt{m^2 + 2eBn}} \right) + \mathcal{M}_{0e},$$



$$\mathcal{M}_W = -\frac{\Omega_W}{B} + \frac{e^2 B}{8\pi^2} \left[\int_{-\infty}^{\infty} \frac{dp_3}{\epsilon_q^0} (n_{0p}^+ + n_{0p}^-) \right] + \mathcal{M}_{0W}$$

$$T_{\mu\nu} = \langle \mathcal{T}_{\mu\nu} \rangle_s,$$

$$-\frac{e^2 B}{4\pi^2} \sum_0^{\infty} b_n \left(n + \frac{1}{2} \right) \left[\int_{-\infty}^{\infty} \frac{dp_3}{\epsilon_q} (n_p^+ + n_p^-) \right]$$

$$\mathcal{T}_{\mu\nu} = \frac{\delta \mathcal{L}}{\delta A_{\mu\nu}^a} A_{\mu\nu}^a - \delta_{\mu\nu} \mathcal{L}$$

$$p_3 = -\Omega, \quad p_{\perp} = -\Omega - B\mathcal{M}$$

$$\mathcal{M}_e = \frac{e}{2\pi^2} \left(\mu_e \sqrt{\mu_e^2 - m^2} - m^2 \ln \frac{\mu_e + \sqrt{\mu_e^2 - m^2}}{m} \right)$$

$$\mu_e \simeq \sqrt{(2\pi^2 N_e / eB)^2 + m^2}$$

$$p_{\perp} = -\Omega_e - B\mathcal{M}_e = 0.$$

$$n_{\mu} = I \left(\frac{\mu_e^2 - m^2}{2eB} \right) = \frac{2\pi^4 N_e^2}{e^3 B^3} \sim 4.75 \times 10^{-20} \frac{N_e^2}{B^3}$$

We conclude, first, that if a degenerate electron gas is confined to its Landau ground state, its transverse pressure vanishes. This phenomenon establishes a limit to the magnetic fields expected to be observable in white dwarfs, and even in neutron stars. Second, the instability of the vacuum in magnetic fields $B \sim B_c$ in a hot and dense medium, is avoided, since the self-consistent magnetization prevents fields greater than $2B_c/3$, although under such conditions the system becomes also unstable and collapses.



Leptonic CP violation in a two parameter model

We further study the “complementary” ansatz, $\text{Tr}(M_\nu) = 0$, for a prediagonal light Majorana type neutrino mass matrix. Previously, this was studied for the CP conserving case and the case where the two Majorana type CP violating phases were present but the Dirac type CP violating phase was neglected. Here we employ a simple geometric algorithm which enables us to “solve” the ansatz including all three CP violating phases. Specifically, given the known neutrino oscillation data and an assumed two parameter (the third neutrino mass m_3 and the Dirac CP phase δ) family of inputs we predict the neutrino masses and Majorana CP phases. Despite the two parameter ambiguity, interesting statements emerge. There is a characteristic pattern of interconnected masses and CP phases. For large m_3 the three neutrinos are approximately degenerate. The only possibility for a mass hierarchy is to have m_3 smaller than the other two. A hierarchy with m_3 largest is not allowed. Small CP violation is possible only near two special values of m_3 . Also, the neutrinoless double beta decay parameter is approximately bounded as $0.020 \text{ eV} < |m_{ee}| < 0.185 \text{ eV}$. As a by-product of looking at physical amplitudes we discuss an alternative parametrization of the lepton mixing matrix which results in simpler formulas. The physical meaning of this parametrization is explained.

S. S. Masood, S. Nasri and J. Schechter, *Phys. Rev. D* **71**, 093005 (2005).



Parametrization

$$K = K_{\text{exp}} \omega_{\tau}^{-1}(\tau),$$

$$\mathcal{L} = \frac{ig}{\sqrt{2}} W_{\mu}^{-} \bar{e}_L \gamma_{\mu} K \nu + \text{H.c.}$$

$$\omega_0(\tau) = \text{diag}(e^{i\tau_1}, e^{i\tau_2}, e^{i\tau_3}), \quad \tau_1 + \tau_2 + \tau_3 = 0.$$

$$K_{\text{exp}} = \omega_{23}(\theta_{23}, 0) \omega_{13}(\theta_{13}, -\delta) \omega_{12}(\theta_{12}, 0),$$

$$\omega_{12}(\theta_{12}, \phi_{12}) = \begin{bmatrix} \cos\theta_{12} & e^{i\phi_{12}} \sin\theta_{12} & 0 \\ -e^{-i\phi_{12}} \sin\theta_{12} & \cos\theta_{12} & 0 \\ 0 & 0 & 1 \end{bmatrix}$$

$$K_{\text{exp}} = \begin{bmatrix} c_{12}c_{13} & s_{12}c_{13} & s_{13}e^{-i\delta} \\ -s_{12}c_{23} - c_{12}s_{13}s_{23}e^{i\delta} & c_{12}c_{23} - s_{12}s_{13}s_{23}e^{i\delta} & c_{13}s_{23} \\ s_{12}s_{23} - c_{12}s_{13}c_{23}e^{i\delta} & -c_{12}s_{23} - s_{12}s_{13}c_{23}e^{i\delta} & c_{13}c_{23} \end{bmatrix}$$

$$\cos\mu'_1 = \frac{-(m'_1)^2 + (m'_2)^2 + (m'_3)^2}{2m'_2 m'_3}.$$

$$A \equiv m_2^2 - m_1^2 = 6.9 \times 10^{-5} eV^2,$$

$$s_{12}^2 = 0.30, \quad s_{23}^2 = 0.50, \quad s_{13}^2 \leq 0.047,$$

$$B \equiv |m_3^2 - m_2^2| = 2.6 \times 10^{-3} eV^2.$$

$$G_1 = [1 - 4(c_{12}s_{13})^2 \sin^2 \delta + 4(c_{12}s_{13})^4 \sin^2 \delta]^{1/2},$$

$$G_2 = [1 - 4(s_{12}s_{13})^2 \sin^2 \delta + 4(s_{12}s_{13})^4 \sin^2 \delta]^{1/2},$$

$$G_3 = [1 - 4s_{13}^2 \sin^2 \delta + 4s_{13}^4 \sin^2 \delta]^{1/2}.$$

Auxiliary masses $m'_i = G_i m_i,$

$$F_1 = \frac{1}{2} \arctan \frac{(c_{12}s_{13})^2 \sin(2\delta)}{1 - 2(c_{12}s_{13})^2 \sin^2 \delta},$$

$$F_2 = \frac{1}{2} \arctan \frac{(s_{12}s_{13})^2 \sin(2\delta)}{1 - 2(s_{12}s_{13})^2 \sin^2 \delta},$$

$$F_3 = -\frac{1}{2} \arctan \frac{s_{13}^2 \sin(2\delta)}{1 + 2s_{13}^2 \sin^2 \delta}.$$

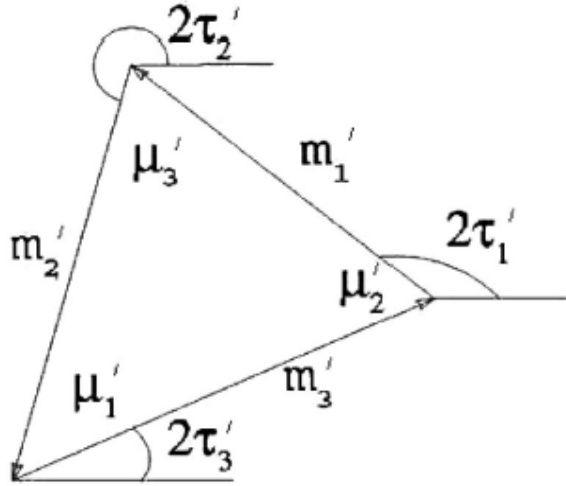
Physical Phases $\tau_i = \tau'_i + F_i$ $m_2^2 = A + m_1^2,$

$$m_1^2 = m_3^2 - A \mp B,$$



$$\text{Tr}(\hat{M}_\nu K_{\text{exp}}^{-1} K_{\text{exp}}^* \omega_0(2\tau)) = 0,$$

$$m'_1 e^{2i\tau'_1} + m'_2 e^{2i\tau'_2} + m'_3 e^{2i\tau'_3} = 0.$$



$$m_1 e^{2i\tau_1} [1 - 2i(c_{12}s_{13})^2 \sin\delta e^{-i\delta}] \\ + m_2 e^{2i\tau_2} [1 - 2i(s_{12}s_{13})^2 \sin\delta e^{-i\delta}] \\ + m_3 e^{2i\tau_3} [1 + 2i(s_{13})^2 \sin\delta e^{i\delta}] = 0.$$

$$\tau'_1 = \frac{1}{6}(\pi - \mu'_1 - 2\mu'_2) + \rho,$$

$$\tau'_2 = \frac{1}{6}(\pi + 2\mu'_1 + \mu'_2) + \rho,$$

$$\tau'_3 = \frac{1}{6}(-2\pi - \mu'_1 + \mu'_2) + \rho.$$

$$\cos\mu'_1 = \frac{-(m'_1)^2 + (m'_2)^2 + (m'_3)^2}{2m'_2 m'_3}.$$

$$|m_1| + |m_2| + |m_3| < 0.7 \text{ eV}.$$

$\sum_i \tau_i = 0$. implies $\rho = -\frac{1}{3} \sum_i F_{\nu}$ Because there is no constraint on $\sum_i \tau'_i$.

S. S. Masood, S. Nasri and J. Schechter, *Phys. Rev. D* 71, 093005 (2005).



TABLE I. Panorama of solutions as m_3 is lowered from about the highest value which is experimentally reasonable to about the lowest value imposed by the model. For each value of m_3 , predictions are given for (m_1, m_2) and for (τ_1, τ_2) in the cases where $\delta = 0, 0.5, 1.0, 1.5, 2.0, 2.5$. All phases are measured in radians. Here the value $s_{13}^2 = 0.04$ was adopted. In the type I solutions m_3 is the largest mass while in the type II solutions m_3 is the smallest mass.

| Type | m_1, m_2, m_3 in eV | $\tau_1, \tau_2(\delta = 0)$ | $\tau_1, \tau_2(\delta = 0.5)$ | $\tau_1, \tau_2(\delta = 1.0)$ | $\tau_1, \tau_2(\delta = 1.5)$ | $\tau_1, \tau_2(\delta = 2.0)$ | $\tau_1, \tau_2(\delta = 2.5)$ |
|------|-----------------------|------------------------------|--------------------------------|--------------------------------|--------------------------------|--------------------------------|--------------------------------|
| I | 0.2955, 0.2956, 0.3 | 0.0043, 1.0428 | 0.0126, 1.0495 | 0.0058, 1.0536 | -0.0108, 1.0510 | -0.0210, 1.0440 | -0.0153, 1.0394 |
| II | 0.3042, 0.3043, 0.3 | -0.0041, 1.0512 | 0.0043, 1.0577 | -0.0023, 1.0615 | -0.0189, 1.0587 | -0.0291, 1.0518 | -0.0235, 1.0476 |
| I | 0.0856, 0.0860, 0.1 | 0.0486, 0.9975 | 0.0566, 1.0049 | 0.0489, 1.0106 | 0.0318, 1.0091 | 0.0219, 1.0015 | 0.0285, 0.9953 |
| II | 0.1119, 0.1123, 0.1 | -0.0311, 1.0774 | -0.0226, 1.0835 | -0.0289, 1.0863 | -0.0453, 1.0828 | -0.0556, 1.0763 | -0.0503, 1.0731 |
| I | 0.0305, 0.0316, 0.06 | 0.3913, 0.6543 | 0.3873, 0.6748 | 0.3578, 0.7048 | 0.3288, 0.7167 | 0.3258, 0.7013 | 0.3530, 0.6720 |
| II | 0.0783, 0.0787, 0.06 | -0.0669, 1.1119 | -0.0583, 1.1174 | -0.0644, 1.1188 | -0.0806, 1.1145 | -0.0911, 1.1085 | -0.0860, 1.1066 |
| II | 0.0643, 0.0648, 0.04 | -0.1064, 1.1494 | -0.0978, 1.1541 | -0.1040, 1.1538 | -0.1203, 1.1483 | -0.1307, 1.1430 | -0.1255, 1.1428 |
| II | 0.0541, 0.0548, 0.02 | -0.1747, 1.2115 | -0.1669, 1.2142 | -0.1751, 1.2095 | -0.1928, 1.2012 | -0.2024, 1.1976 | -0.1951, 1.2019 |
| II | 0.0506, 0.0512, 0.005 | -0.2601, 1.2620 | -0.2603, 1.2611 | -0.2914, 1.2276 | -0.3251, 1.2035 | -0.3250, 1.2094 | -0.2950, 1.2369 |
| II | 0.0503, 0.0510, 0.001 | -0.3830, 1.1805 | | | | | |

Table I shows that at this value both type I and type II solutions exist. This is true also for higher values of m_3 . The picture remains very similar down to around $m_3 = 0.1$ eV but as one gets closer to roughly 0.06 eV, there is a marked change. If one further lowers m_3 , it is found that the type I solution no longer exists. On the other hand the type II solution persists and does not change much until m_3 approaches the neighborhood of 0.001 eV. There are no solutions for m_3 below this region.



TABLE II. Minimum allowed value of the input mass m_3 as a function of the input CP violation phase δ . These correspond to the cases where the triangle in Fig. 1 becomes degenerate. Here, the choice $s_{13}^2 = 0.04$ has been made.

| Type | $(m_3)_{\min} (\delta = 0)$ in eV | $(m_3)_{\min} (\delta = 0.5)$ | $(m_3)_{\min} (\delta = 1.0)$ | $(m_3)_{\min} (\delta = 1.5)$ | $(m_3)_{\min} (\delta = 2.0)$ | $(m_3)_{\min} (\delta = 2.5)$ |
|------|-----------------------------------|-------------------------------|-------------------------------|-------------------------------|-------------------------------|-------------------------------|
| I | 0.059 271 6 | 0.059 096 7 | 0.058 717 8 | 0.058 479 9 | 0.058 620 3 | 0.058 997 1 |
| II | 0.000 681 1 | 0.001 0546 1 | 0.001 902 4 | 0.002 463 6 | 0.002 129 4 | 0.001 272 3 |

$$0.020 \text{ eV} < |m_{ee}| < 0.185 \text{ eV}.$$

TABLE III. Panorama of solutions, using the reflected triangle, as m_3 is lowered from about the highest value which is experimentally reasonable to about the lowest value imposed by the model. Notice that the predicted masses m_1 and m_2 have not been given since they are the same as in Table I.

| Type | m_3 in eV | $\tau_1, \tau_2(\delta = 0)$ | $\tau_1, \tau_2(\delta = 0.5)$ | $\tau_1, \tau_2(\delta = 1.0)$ | $\tau_1, \tau_2(\delta = 1.5)$ | $\tau_1, \tau_2(\delta = 2.0)$ | $\tau_1, \tau_2(\delta = 2.5)$ |
|------|-------------|------------------------------|--------------------------------|--------------------------------|--------------------------------|--------------------------------|--------------------------------|
| I | 0.3 | -0.0043, -1.0428 | 0.0113, -1.0393 | 0.0210, -1.0422 | 0.0151, -1.0492 | -0.0015, -1.0536 | -0.0123, -1.0512 |
| II | 0.3 | 0.0041, -1.0512 | 0.0196, -1.0475 | 0.0291, -1.0500 | 0.0232, -1.0569 | 0.0066, -1.0614 | -0.0040, -1.0593 |
| I | 0.1 | -0.0486, -0.9975 | -0.0326, -0.9947 | -0.0221, -0.9992 | -0.0275, -1.0073 | -0.0444, -1.0111 | -0.0560, -1.0070 |
| II | 0.1 | 0.0311, -1.0774 | 0.0465, -1.0732 | 0.0557, -1.0748 | 0.0495, -1.0810 | 0.0331, -1.0859 | 0.0228, -1.0848 |
| I | 0.06 | -0.3913, -0.6543 | -0.3634, -0.6645 | -0.3310, -0.6934 | -0.3246, -0.7149 | -0.3483, -0.7109 | -0.3806, -0.6837 |
| II | 0.06 | 0.0669, -1.1119 | 0.0822, -1.1071 | 0.0912, -1.1073 | 0.0849, -1.1127 | 0.0685, -1.1180 | 0.0584, -1.1183 |
| II | 0.04 | 0.1064, -1.1494 | 0.1217, -1.1438 | 0.1308, -1.1423 | 0.1246, -1.1465 | 0.1082, -1.1526 | 0.0979, -1.1506 |
| II | 0.02 | 0.1747, -1.2115 | 0.1909, -1.2040 | 0.2019, -1.1981 | 0.1971, -1.1994 | 0.1799, -1.2072 | 0.1676, -1.2136 |
| II | 0.005 | 0.2601, -1.2620 | 0.2853, -1.2447 | 0.3182, -1.2162 | 0.3294, -1.2017 | 0.3024, -1.2190 | 0.2694, -1.2486 |
| II | 0.001 | 0.3830, -1.1805 | | | | | |

TABLE IV. Panorama of solutions as in Table I but with $s_{13}^2 = 0.01$. Notice that the predicted masses m_1 and m_2 have not been given since they are the same as in Table I.

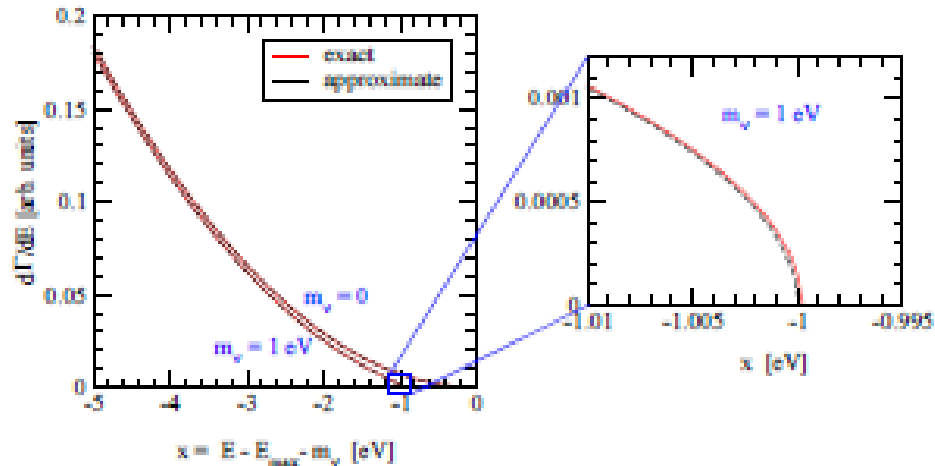
| Type | m_3 in eV | $\tau_1, \tau_2(\delta = 0)$ | $\tau_1, \tau_2(\delta = 0.5)$ | $\tau_1, \tau_2(\delta = 1.0)$ | $\tau_1, \tau_2(\delta = 1.5)$ | $\tau_1, \tau_2(\delta = 2.0)$ | $\tau_1, \tau_2(\delta = 2.5)$ |
|------|-------------|------------------------------|--------------------------------|--------------------------------|--------------------------------|--------------------------------|--------------------------------|
| I | 0.3 | -0.0043, -1.0428 | 0.0063, 1.0445 | 0.0046, 1.0455 | 0.0007, 1.0448 | -0.0018, 1.0432 | -0.0006, 1.0420 |
| II | 0.3 | 0.0041, -1.0512 | -0.0020, 1.0528 | -0.0037, 1.0537 | -0.0076, 1.0530 | -0.0101, 1.0514 | -0.0089, 1.0503 |
| I | 0.1 | -0.0486, -0.9975 | 0.0505, 0.9994 | 0.0486, 1.0008 | 0.0446, 1.0004 | 0.0421, 0.9985 | 0.0436, 0.9970 |
| II | 0.1 | 0.0311, -1.0774 | -0.0290, 1.0789 | -0.0306, 1.0796 | -0.0345, 1.0787 | -0.0370, 1.0772 | -0.0358, 1.0763 |
| I | 0.06 | -0.3913, -0.6543 | 0.3900, 0.6597 | 0.3816, 0.6681 | 0.3738, 0.6718 | 0.3736, 0.6676 | 0.3813, 0.6592 |
| II | 0.06 | 0.0669, -1.1119 | -0.0608, 1.1132 | -0.0634, 1.1136 | -0.0702, 1.1125 | -0.0727, 1.1111 | -0.0716, 1.1106 |
| II | 0.04 | 0.1064, -1.1494 | -0.1043, 1.1505 | -0.1058, 1.1504 | -0.1097, 1.1492 | -0.1122, 1.1479 | -0.1111, 1.1478 |
| II | 0.02 | 0.1747, -1.2115 | -0.1728, 1.2122 | -0.1748, 1.2110 | -0.1789, 1.2091 | -0.1813, 1.2082 | -0.1797, 1.2091 |
| II | 0.005 | 0.2601, -1.2620 | -0.2605, 1.2602 | -0.2673, 1.2538 | -0.2744, 1.2486 | -0.2750, 1.2496 | -0.2687, 1.2558 |
| II | 0.001 | 0.3830, -1.1805 | 0.4036, 1.1593 | -0.4828, 1.0840 | | | -0.4252, 1.1420 |



Exact relativistic beta decay endpoint spectrum

The exact relativistic form for the beta decay endpoint spectrum is derived and presented in a simple factorized form. We show that our exact formula can be well approximated to yield the endpoint form used in the fit method of the KATRIN collaboration. We also discuss the three neutrino case and how information from neutrino oscillation experiments may be useful in analyzing future beta decay endpoint experiments.

$$\frac{d\Gamma}{dE_e} = \frac{p_e M B}{(2\pi)^3 4(m_{12})^4} (ME_e - m_e^2) \sqrt{y \left(y + \frac{2m_\nu M'}{M} \right)} \left[y + \frac{m_\nu}{M} (M' + m_\nu) \right]$$



$$(ME_e - m_e^2) \rightarrow (ME_e - E_e^2)$$

Figure 1: Comparison of approximate and exact formula



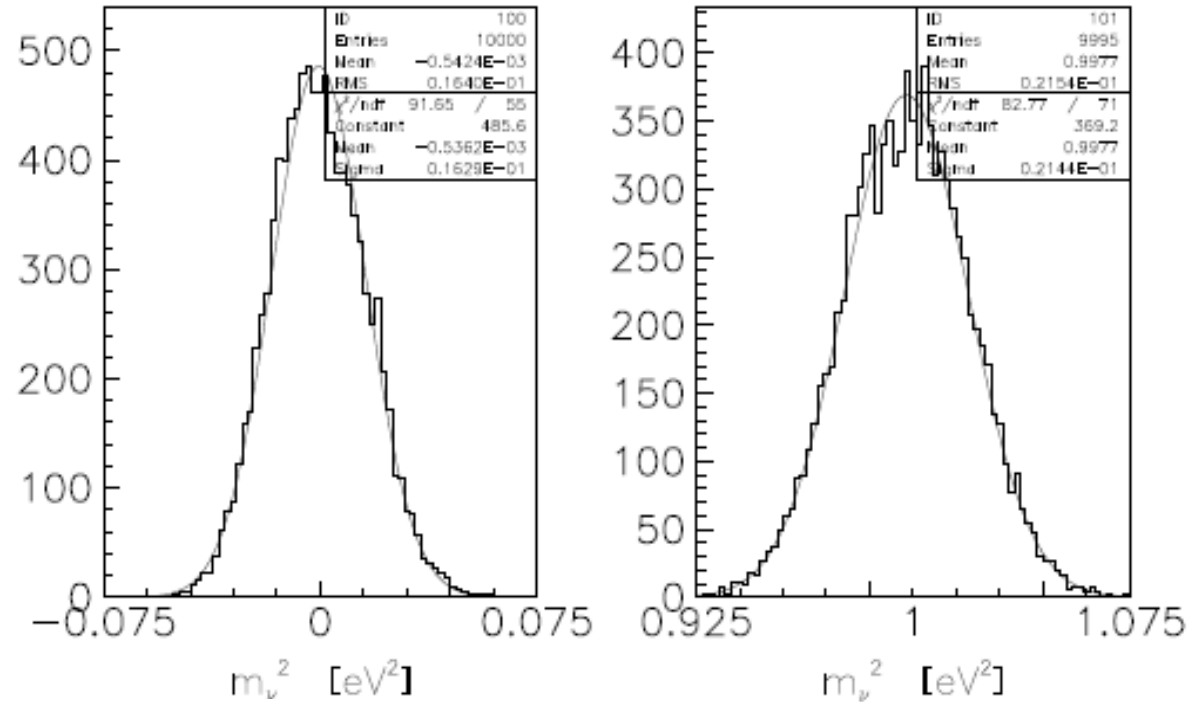
Monte Carlo Simulations of Relativistic Decay rate

An expected background rate of 0.01 s^{-1} .

$$\frac{d\Gamma}{dE_e} \propto (E_0 - V_i - E) \sqrt{(E_0 - V_i - E)^2 - m_\nu^2}.$$

Fig. shows the results for the observable m_ν^2 obtained from the fitting of 10000 sets of MonteCarlo data randomized according to the exact relativistic formula

A signal rate from a KATRIN-like molecular gaseous windowless tritium source with a column density of $5 \cdot 10^{17}$ molecules/cm² over an active area of 53 cm² and an accepted solid angle of $\Delta\Omega/4\pi = 0.18$



A response function of a KATRIN-like experiment considering the energy losses within the tritium source and the main spectrometer transmission function with a total width of 0.93 eV.

The rms values of the Gaussian-like distributions correspond to the expected statistical uncertainty Δm_{stat} for a KATRIN-like experiment.



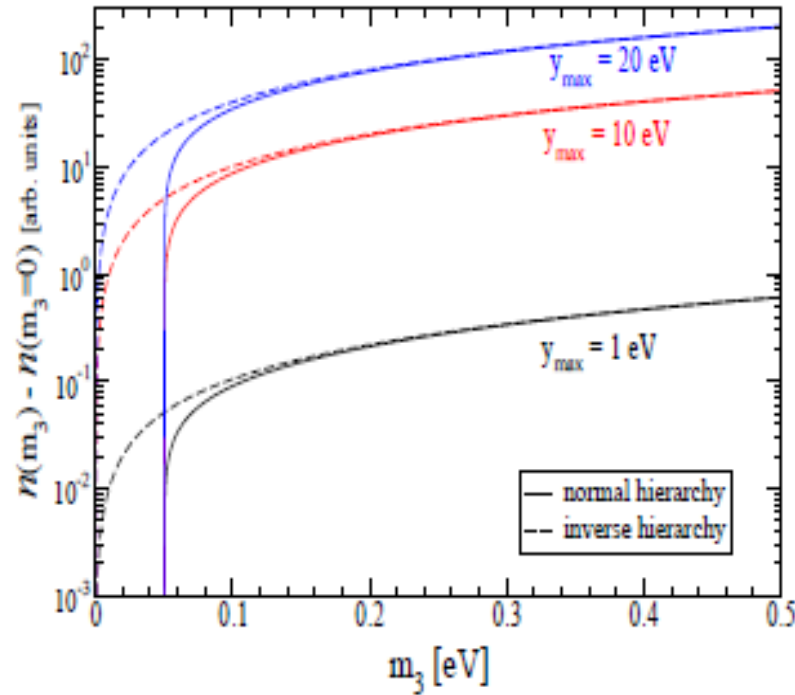
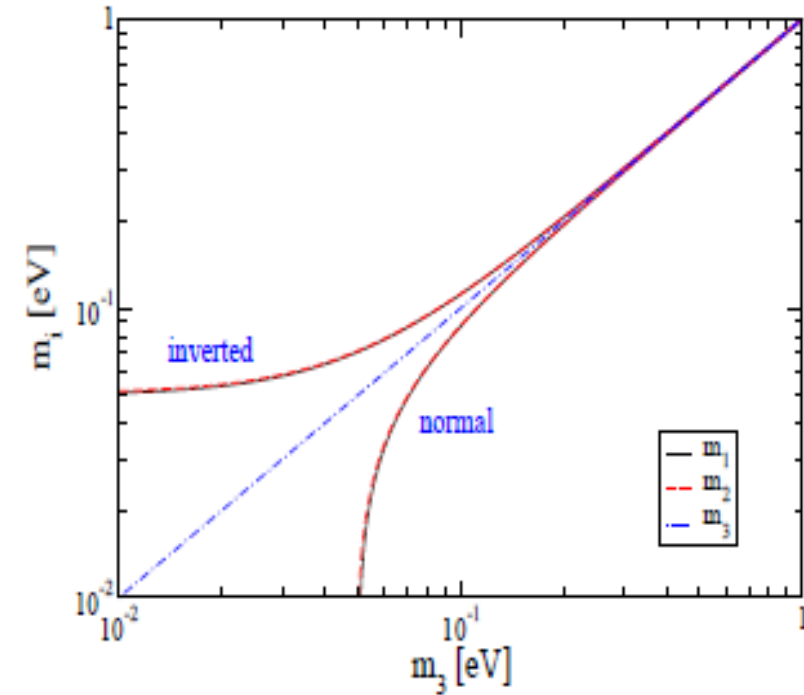
$$A \equiv m_2^2 - m_1^2 = 7.9 \times 10^{-5} eV^2,$$

$$B \equiv |m_3^2 - m_2^2| = 2.6 \times 10^{-3} eV^2,$$

$$|K_{11}|^2 = 0.67,$$

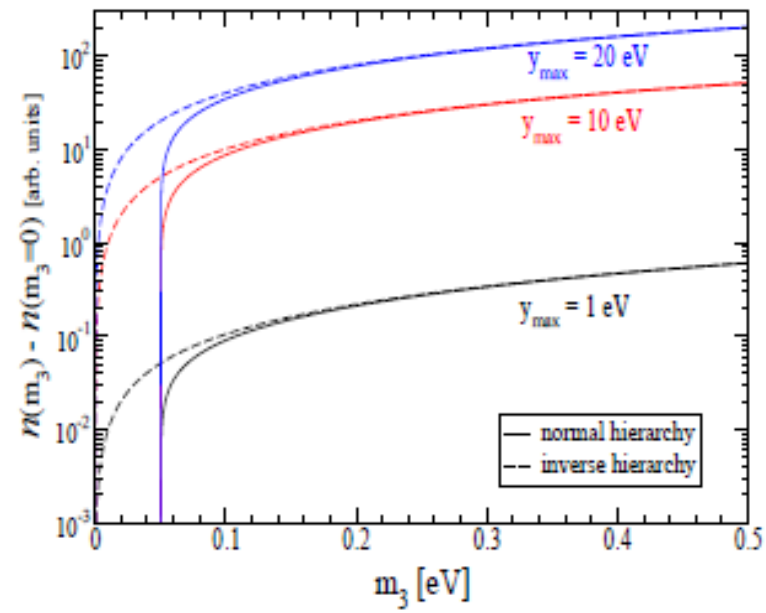
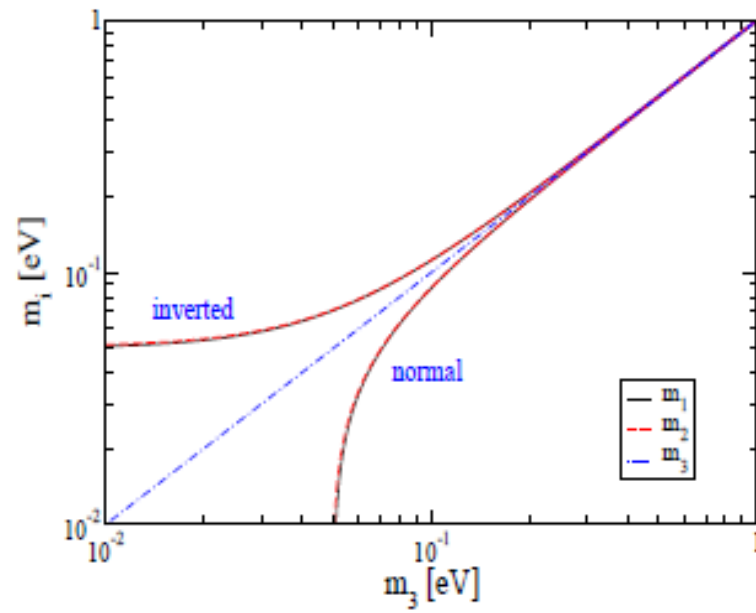
$$|K_{12}|^2 = 0.29,$$

$$|K_{13}|^2 = 0.04.$$



The left panel shows typical solutions for (m_1 , m_2) as a function of m_3 for the NH case (solid curves) and the IH case (dashed curves); the middle dot-dashed is given for orientation. The right panel give the predictions for the quantities, $n(y_{max})$, proportional to the event counting rate which includes emitted electrons within, respectively 1 eV, 10 eV and 20 eV from the appropriate endpoint.





The left panel shows typical solutions for (m_1, m_2) as a function of m_3 for the NH case (solid curves) and the IH case (dashed curves); the middle dot-dashed is given for orientation. The right panel give the predictions for the quantities, $n(y_{\max})$, proportional to the event counting rate which includes emitted electrons within, respectively 1 eV, 10 eV and 20 eV from the appropriate endpoint.



We have derived the exact relativistic form for the beta decay endpoint spectrum and presented it in a very simple and useful factorized form. We showed that our exact formula can be well approximated to yield the endpoint form used in the fit method of the KATRIN collaboration. This was explicitly established through a detailed numerical simulation. We have also discussed the three neutrino case and shown how information from neutrino oscillation experiments may be useful in analyzing future beta decay endpoint experiments.



Summary

- Development of Statistical Quantum Field Theories (SQFT)
- Real-time Formalism and Imaginary-time Formalism
- Renormalization in SQFT (Charge, Mass and Wavefunction of electron)
- Propagation of light in a medium and its properties.
- How light can provide information about electromagnetic properties of a medium
- Modifications in electromagnetic properties of particles in hot and dense media
- Properties of neutrinos in a medium and form factors
- Electromagnetic properties and effective mass of neutrinos in a medium
- Effective mass of Weyl neutrino and its coupling with magnetic field
- Quantum magnetic collapse of neutron star
- Using CP violation parameter, finding a limit on double beta decay
- Relativistic relation is used to find the end point spectrum of beta decay

